



PROCUREMENT EXECUTIVE, MINISTRY OF DEFENCE

AERONAUTICAL RESEARCH COUNCIL

CURRENT PAPERS

A Theoretical Investigation of High-Speed Axisymmetric
Turbulent Mixing Layers with Large Temperature Differences

by

P.W. Carpenter

Department of Engineering Science

University of Exeter

LONDON: HER MAJESTY'S STATIONERY OFFICE

1976

£1.80 net

A THEORETICAL INVESTIGATION OF HIGH-SPEED AXISYMMETRIC
TURBULENT MIXING LAYERS WITH LARGE TEMPERATURE DIFFERENCES

- by -

P.W. Carpenter
Department of Engineering Science,
University of Exeter

SUMMARY

A two-parameter integral method is developed for predicting the mean-flow characteristics of high-speed axisymmetric turbulent mixing layers with large temperature differences. Results are presented graphically and in tabular form for such quantities as spreading rate, entrainment velocity, potential-core length and velocity along the dividing streamline. These results are for the case of a jet issuing into a quiescent medium; a range of jet Mach numbers from 0 to 5 is taken. For each Mach number results are presented corresponding to values of the temperature ratio across the mixing layer ranging from 0 to ∞ . On the whole the available experimental data agree well with the theoretical predictions. Results for the case where the jet issues into a moving stream are not presented graphically or in tabular form, but approximate analytical formulae are given whereby most of the quantities of interest may be determined.

1. Introduction.

The mixing layer at the initial stages of a turbulent jet has been the subject of an enormous number of theoretical and experimental investigations. This great interest is partly generated because the two-dimensional mixing layer is one of the simplest manifestations of turbulent shear flow and consequently is highly suitable for a study of basic processes. However the fact that a wide range of engineering applications involve mixing layers is probably an even more important factor in promoting an interest in them.

The basic properties of hot compressible jets are important in aircraft propulsion (e.g. their effect on jet noise) and in combustion processes. Cold jets exhausting into a hot medium can arise when secondary air is fed into furnaces and combustion chambers. In addition to their role in the initial stages of jet development, mixing layers are also an important component of the flow field for many separated-flow phenomena. The flow over rearward- and forward-facing steps, blunt-based aerofoils and bodies, and over rectangular cavities are typical examples. Indeed, a well-known method of approach due to Chapman (1950) and Korst (1956) assumes that the processes in the mixing layer dominate the entire flow field in such phenomena. There are a wide variety of additional industrial and meteorological applications of turbulent mixing layers.

A relatively simple method for predicting the basic properties of the mixing-layer region in an axisymmetric turbulent jet is described below. The basic properties in question include the spreading rate, potential-core length, entrainment velocity, and dividing-streamline velocity. Results are presented for jet Mach numbers M_J ranging from 0 to 5.0 and for stagnation enthalpy ratios, H_∞/H_J , ranging from 0 to ∞ .

Since/

Since mixing layers have been so widely studied, these results cannot be highly original. However, experimental data for most of the Mach-number and total-enthalpy-ratio range are non-existent or extremely scarce. Engineers are therefore forced to rely on theoretical predictions. It is believed that the results presented below are the first that systematically cover the entire range of interest in Mach number and total-enthalpy ratio. Another objective is to show how the properties of such mixing layers have a behaviour which can be explained with reference to simple physical processes. A short review of previous theoretical investigations is given below.

2. Review of previous theoretical investigations.

The notation is defined in Fig. 1. ρ is the gas density and T is the temperature.

Low speed axisymmetric turbulent mixing layers with $T_J \neq T_\infty$ have been studied theoretically by Szablewski. He used the Prandtl (1942)-Görtler (1942) eddy-viscosity model, assumed that the turbulent Prandtl number $Pr_T = 0,5$ and neglected viscous dissipation. His work is presented in a series of articles. In Szablewski (1957), Görtler's (1942) solution is extended to heated mixing layers, and is used to start an iterative procedure for finding numerical solutions of the two-dimensional case with $(T_J + T_\infty)/T_\infty = 0, 1, 2, 5$ and $(u_J - u_\infty)/u_J = 0, 0,25, 0,5, 0,75, 1$. The corresponding axisymmetric mixing layers are studied in Szablewski (1958) $\{(u_J - u_\infty)/u_J = 0, 0,25, 0,5, 0,75\}$ and Szablewski (1961) $\{(u_J - u_\infty)/u_J = 1\}$. Finally, Szablewski (1963) considered the case of a cool jet issuing into a hot medium $\{(T_J - T_\infty)/T_\infty = -0,25, -0,5, -0,75\}$.

Compressible heated mixing layers have been considered by several investigators, notably Crane (1957) {asymptotic expansion technique, $Pr_T = 1$ }, Jacques and Gailly (1966) {numerical solution, $Pr_T = 1, 0 \leq M_J \leq 4,0$ } and Mills (1968) {numerical solution, $Pr_T = 0,5, 0 \leq M_J \leq 5,0, 0,2 \leq T_\infty/T_J \leq 0,8$ }. These investigators confined themselves in the main to predicting the velocity-profile shape.

There have also been two series of investigators who linearized the equations of motion {after the fashion of Görtler (1942) and Pai (1949)} to obtain approximate solutions. One series consisted of Korst and his co-workers e.g. Korst et al. (1954) and Korst and Chow (1966). The other series starts with Libby (1962), continues to Alpinieri (1964), through Kleinstein (1964) to Cook and Singer (1969). Each investigator used a different eddy-viscosity model, and each is primarily concerned with the main part of jets issuing into streams of different gases.

Also, there are the series of investigations based on Warren's (1957) integral method; Warren gave results for $0 \leq M_J \leq 2,6$ and $0,25 \leq H_\infty/H_J \leq 1$. The method was extended to inhomogeneous mixing layers by Donaldson and Gray (1966), and to the $(u_\infty \neq 0)$ case by Smoot and Purcell (1967).

Finally, Abramovich's (1963) integral method should be mentioned. The basic premise of this rather crude technique is an assumed variation of spreading rate with density; the spreading rate is not actually calculated.

Despite this very considerable effort, the influence of compressibility and heat transfer on the basic properties, especially entrainment velocity, has still not been adequately determined.

3. Choice of eddy-viscosity model and value for turbulent Prandtl number.

Traditional eddy-viscosity models have proved inadequate for many turbulent shearflow phenomena. This situation has led to the development of the turbulent-energy methods, e.g. Bradshaw et al. (1967). Nevertheless, the velocity profile in incompressible mixing layers is predicted very satisfactorily using the Prandtl-Görtler model, viz.

$$-\overline{\rho u'v'} = \kappa \bar{\rho} (u_J - u_\infty) b \partial \bar{u} / \partial r \quad (3.1)$$

where u' and v' are the fluctuating velocity components in the x and r directions respectively, \bar{u} is the mean axial velocity, b is the mixing-layer thickness and κ is a constant (a kind of inverse turbulent Reynolds number). Therefore there is little point in adopting a more sophisticated model for the problem in hand.

The major difficulty is how to take into account the effect of compressibility and heat transfer on the kinematic eddy viscosity. Many investigators have used a transformation technique {e.g. Ting and Libby (1960), Channapragada (1963), Channapragada and Wooley (1967), and Laufer (1969)}; others have replaced b in eqn. (3.1) by a density-dependent thickness or have assumed a particular functional dependence of κ on the mean density {e.g. Ferri et al. (1962), Alpinieri (1964) and Schetz (1968)}. However, these methods lead to velocity profiles that are at variance with experimental ones, which invariably are little different in shape from incompressible ones {e.g. see Hill and Nicholson (1964) who compare measured profiles to various theoretical predictions}.

Morkovin (1962) suggested that the turbulence structure in turbulent shear layers would be unaffected by compressibility providing the fluctuations in Mach number were less than unity. This hypothesis, or deductions therefrom, appears to work well for compressible boundary layers {e.g. see Bradshaw (1967), Maise and McDonald (1968), Herring and Mellor (1968), and Bradshaw and Ferris (1971)}. In jets the velocity and density fluctuations are much larger than in boundary layers. In view of this Morkovin's hypothesis would be expected to fail in jets for Mach numbers which exceed one or two. Consequently, the variation of κ with Mach number and total-enthalpy ratio is deduced by fitting theoretical predictions to the experimental data for spreading rate. The available experimental evidence discussed in Section 5 suggests that κ remains approximately constant with change in total-enthalpy ratio but probably decreases with a rise in jet Mach number.

The question of choosing a value for the turbulent Prandtl number is now considered. Unlike its molecular counterpart, the turbulent Prandtl number is not a property of the fluid, but rather a property of a particular flow field. There is no reason for it to be the same for different shear flows, or even to be constant across a particular mixing layer. However, if for simplicity it is assumed constant, what value should it take? The experimental evidence is somewhat confusing. Hinze and Zijnen's (1948) measurements in a low speed jet show Pr_T varying from 0.70 at the centre-line to 1.25 at the edge. Broer and Rietdijk (1960) report similar values in an ($M_J = 1.74$) jet. Pabst (1960) and Corrsin and Uberoi (1950) report $Pr_T = 0.70$

for hot mixing layers. A plasma jet of $M_J = 2.35$ and $T_J/T_\infty = 10.4$ was found by Demetriades and Doughman (1969) to have $Pr_T = 0.89$. If Pr_T is chosen as unity, considerable theoretical simplification is achieved, and on the face of it this does not seem a bad choice although the evidence reviewed above suggests 0.7 is the best choice.

4. Analysis.

(i) Governing equations.

The governing equations for compressible turbulent mixing layers may be written in the following form,

$$\frac{\partial}{\partial x} (\bar{\rho} \bar{u}) + \frac{1}{r} \frac{\partial}{\partial r} (r \bar{\rho} \bar{v}) = 0 \quad (4.1)$$

$$\bar{\rho} \bar{u} \frac{\partial \bar{u}}{\partial x} + \bar{\rho} \bar{v} \frac{\partial \bar{u}}{\partial r} = \frac{1}{r} \frac{\partial}{\partial r} (r \bar{\rho} \epsilon \frac{\partial \bar{u}}{\partial r}) \quad (4.2)$$

$$\begin{aligned} \bar{\rho} \bar{u} \frac{\partial \bar{H}}{\partial x} + \bar{\rho} \bar{v} \frac{\partial \bar{H}}{\partial r} &= \frac{1}{r} \frac{\partial}{\partial r} \left\{ \frac{\epsilon}{Pr_T} r \frac{\partial \bar{H}}{\partial r} \right\} \\ &\quad - \frac{1}{2r} \frac{\partial}{\partial r} \left\{ \left(\frac{1}{Pr_T} - 1 \right) \epsilon r \frac{\partial \bar{u}^2}{\partial r} \right\} \end{aligned} \quad (4.3)$$

where (u, v) are the velocity components in the (x, r) directions, ρ is the density, a bar indicates time-averaged quantities and where the following definitions apply

$$\bar{v} = \bar{v} \left\{ 1 + \frac{\overline{v'v'}}{(\bar{\rho} \bar{v})} \right\} \quad (a)$$

$$\bar{H} = c_p \bar{T} + \bar{u}^2/2 \quad (b)$$

$$\epsilon = - \frac{\overline{u'v'}}{(\partial \bar{u} / \partial r)} \quad (c)$$

$$Pr_T = \epsilon / \epsilon_T \quad (d)$$

$$\epsilon_T = - \frac{\overline{v'T'}}{(\partial \bar{T} / \partial r)} \quad (e) \quad (4.4)$$

where a dash indicates fluctuating quantities,

The notation is further defined in Fig. 1. The boundary conditions on the governing equations are

$$\left. \begin{aligned} \bar{u} &= u_\infty \\ \bar{H} &= H_\infty \end{aligned} \right\} \text{ for } r > r_2(x) \quad (a)$$

$$\left. \begin{aligned} \bar{u} &= u_J \\ \bar{H} &= H_J \end{aligned} \right\} \text{ for } r < r_1(x) \quad (b)$$

$$\bar{v} = 0 \quad \text{at} \quad r = r_1(x) \quad (c)$$

$$r_1 = r_2 = r_0 \quad \text{at} \quad x = 0 \quad (d) \quad (4.5)$$

Under the boundary-layer approximation the boundary condition (4.5c) is equivalent to $\bar{v} = 0$ at $r = 0$. The position of the inner and outer edges, r_1 and r_2 , are unknown a priori for $x > 0$.

If $Pr_T = 1$ then eqn. (4.3) may be solved to give

$$\bar{H} = H_J - (H_J - H_\infty) (u_J - \bar{u}) / (u_J - u_\infty) \quad (4.6)$$

Non-dimensional density and temperature profiles may be derived from eqn. (4.6) and have the form

$$\frac{\bar{T}}{T_J} = \frac{\rho}{\rho_0} = (1 + m) \left\{ 1 - \frac{1 - \lambda_H}{1 - \lambda} \left(1 - \frac{\bar{u}}{u_J} \right) \right\} - m \left(\frac{\bar{u}}{u_J} \right)^2 \quad (4.7)$$

$$\text{where } m = (\gamma - 1) M_J^2 / 2, \quad \lambda = u_\infty / u_J, \quad \lambda_H = H_\infty / H_J \quad (4.8)$$

and γ is the ratio of the specific heats.

(ii) Derivation of integral relations.

Multiply eqn. (4.1) by a weighting factor $r f_j(\bar{u})$ and eqn. (4.2) by $r f_j'(\bar{u})$, where in this case the dash indicates differentiation with respect to \bar{u} . Integrate the sum of these two products with respect to r from $r = 0$ to ∞ . The result can be written in the form

$$\begin{aligned} \frac{d}{dx} \int_0^\infty \bar{\rho} \bar{u} f_j(\bar{u}) r dr + \bar{\rho} r \bar{v} f_j(\bar{u}) \Big|_0^\infty \\ = r \epsilon \frac{\partial \bar{u}}{\partial r} f_j'(\bar{u}) \Big|_0^\infty - \int_0^\infty \epsilon \left(\frac{\partial \bar{u}}{\partial r} \right)^2 f_j''(\bar{u}) r dr \end{aligned} \quad (4.9)$$

$j = 0, 1, 2, \dots$

Now by symmetry $\bar{v} = 0$ and $\partial \bar{u} / \partial r = 0$ at $r = 0$. Let the $f_j(\bar{u})$ be required to satisfy

$$f_j(u_\infty) = 0; \quad j = 0, 1, 2, \dots \quad (4.10)$$

and let the independent variables be transformed as follows

$$\{ x, r \} \rightarrow \{ \xi = \kappa x / r_0, \quad \zeta = (r - r_1) / b \} \quad (4.11)$$

In addition if it is assumed that $\partial \bar{u} / \partial r = 0$ at $r = r_1$ and r_2 , and finally if eqn. (3.1) is used, then eqn. (4.9) becomes

$$\begin{aligned} & \frac{d}{d\xi} \left\{ \hat{b}^2 \int_0^1 R U f_j(U) \zeta d\zeta + \hat{r}_1 \hat{b} \int_0^1 R U f_j(U) d\zeta + \frac{\hat{r}_1^2}{2} f_j(U) \right\} \\ & = -\hat{b}(1-\lambda) \int_0^1 R \left(\frac{dU}{d\zeta}\right)^2 f_j''(U) \zeta d\zeta - \hat{r}_1(1-\lambda) \int_0^1 R \left(\frac{dU}{d\zeta}\right)^2 f_j''(U) d\zeta \\ & \qquad \qquad \qquad j = 0, 1, \dots \qquad (4.12) \end{aligned}$$

where $R = \bar{\rho}/\rho_j$; $U = \bar{u}/u_j$, $\hat{r}_1 = r_1/r_0$, $\hat{r}_2 = r_2/r_0$ and $\hat{b} = b/r_0$.

(iii) Determination of \hat{b} , \hat{r}_1 and \hat{r}_2 .

To proceed further a functional form must be chosen for U . Many theoretical and experimental studies of mixing layers have shown that the actual shape of the velocity profile is only slightly altered by changes in λ , M_j and λ_H . Therefore it is assumed that U is an invariant function of ζ , and the following functional form is chosen

$$U(\zeta) = (1+\lambda)/2 - \{(1-\lambda)/2\} \tanh(k_1\zeta + k_2) \qquad (4.13)$$

where $k_1 = 2 \operatorname{arctanh}(0.98)$ and $k_2 = -\operatorname{arctanh}(0.98)$. This function is very close to the exact solution for an incompressible mixing layer. In effect, it is a two-parameter family of profiles, \hat{r}_1 and \hat{b} being the two parameters implicit in (4.13). Equation (4.7) may be used to obtain an expression for R .

Since there are two unknown functions (or parameters) of ξ to be determined, two of the integral relations (4.12) are required. The simplest two weighting functions which are linearly independent and satisfy condition (4.10) are

$$f_0 = U - \lambda, \quad f_1 = (U - 1)(U - \lambda) \qquad (4.14)$$

With the substitution of the weighting functions (4.14) in equation (4.12) the following two equations are obtained

$$\frac{d}{d\xi} \left\{ \hat{r}_1^2 \frac{(1-\lambda)}{2} + \hat{b}^2 I_B + \hat{r}_1 \hat{b} J_B \right\} = 0 \qquad (j = 0) \qquad (4.15)$$

$$(2\hat{b} I_A + \hat{r}_1 J_A) \frac{d\hat{b}}{d\xi} + \hat{b} J_A \frac{d\hat{r}_1}{d\xi} = -\hat{b} K_A - \hat{r}_1 L_A \qquad (j = 1) \qquad (4.16)$$

where $I_A = \int_0^1 R U (U-\lambda) (U-1) \zeta d\zeta$, $J_A = \int_0^1 R U (U-\lambda) (U-1) d\zeta$

$$K_A = 2(1-\lambda) \int_0^1 R (dU/d\zeta)^2 \zeta d\zeta, \quad L_A = 2(1-\lambda) \int_0^1 R (dU/d\zeta)^2 d\zeta$$

$$I_B = \int_0^1 RU(U-\lambda)\zeta d\zeta, \quad J_B = \int_0^1 RU(U-\lambda)d\zeta \quad (4.17)$$

Eqn. (4.15) may be integrated to give

$$(\hat{r}_1^2 - 1)(1-\lambda)/2 + \hat{b}^2 I_B + \hat{r}_1 \hat{b} J_B = 0 \quad (4.18)$$

If $\lambda = 0$ and $\xi \rightarrow 0$ ($\hat{b} \rightarrow 0$) the roots of eqn. (4.18) become $\hat{r}_1 = \pm 1$. So obviously only one of the two roots is physically acceptable, this root, which establishes a relationship between \hat{r}_1 and \hat{b} , takes the form

$$\hat{r}_1 = -\hat{b}J_B/(1-\lambda) + \{ 1 + \hat{b}^2 J_B^2 / (1-\lambda)^2 - 2\hat{b}^2 I_B / (1-\lambda) \}^{1/2} \quad (4.19)$$

In principle, one can substitute from eqn. (4.19) in (4.16) and thus the problem is reduced to solving one nonlinear ordinary differential equation for \hat{b} . To solve this differential equation numerically \hat{b} is represented as a polynomial in ξ , i.e.

$$\hat{b} = b_1 \xi + b_2 \xi^2 + b_3 \xi^3 + b_4 \xi^4 \quad (4.20)$$

Using the binomial theorem, eqn. (4.19) may be expanded in powers of \hat{b} , i.e.

$$\hat{r}_1 = -\hat{b}C_1 + 1 + C_2 \hat{b}^2 / 2 - C_2^2 \hat{b}^4 / 8 \quad (4.21)$$

where $C_1 = J_B / (1-\lambda)$; $C_2 = J_B^2 / (1-\lambda)^2 - 2I_B / (1-\lambda)$

Substituting eqn. (4.20) in (4.21) leads to

$$\begin{aligned} \hat{r}_1 = & 1 - C_1 b_1 \xi + \{- C_1 b_2 + C_2 b_1^2 / 2\} \xi^2 + \{- C_1 b_3 + C_2 b_1 b_2\} \xi^3 \\ & + \{- C_2 b_4 + C_2 (2b_1 b_3 + b_2^2) / 2 - C_2^2 b_1^4 / 8\} \xi^4 + \dots \end{aligned} \quad (4.22)$$

Using the definition of C_1 the following expression is obtained from eqn. (4.22) for η_2 { $= \lim_{\xi \rightarrow 0} \left(\frac{r_2 - 1}{\hat{b}} \right)$ }

$$\eta_2 = (\Delta_2 - \lambda \Delta_1) / (1 - \lambda) \quad (4.23)$$

$$\text{where } \Delta_1 = \int_0^1 (1-RU)d\zeta \quad \text{and} \quad \Delta_2 = \int_0^1 (1-RU^2)d\zeta \quad (4.24)$$

η_2 represents the orientation of the outer edge of a two-dimensional mixing layer (or axisymmetric one under the limit $\xi \rightarrow 0$) with respect to a splitter plate (or nozzle $r = r_0$).

By substituting eqn. (4.22) and (4.20) into eqn. (4.16) and equating like powers of ξ , a series of equations for determining b_1 etc. may be obtained in the following form

$$b_1 = -L_A/J_A \quad (4.25)$$

$$b_2 = -\{2b_1^2(I_A - C_1J_A) + b_1(K_A - L_A C_1)\}/(2J_A) \quad (4.26)$$

$$b_3 = -\{3J_A C_2 b_1^3/2 + 6b_1 b_2(I_A - J_A C_1) + b_2(K_A - C_1 L_A) + b_1^2 C_2 L_A/2\}/(3J_A) \quad (4.27)$$

$$b_4 = -\{4b_2^2(I_A - J_A C_1) + 8b_1 b_3(I_A - J_A C_1) + 6b_1^2 b_2 C_2 J_A + b_3(K_A - C_1 L_A) + b_1 b_2 C_2 L_A\}/(4J_A) \quad (4.28)$$

Of course, eqn. (4.25) is equivalent to the two-dimensional result. The polynomial (4.20) is curtailed after the fourth-order term, but this is more than enough to ensure an accuracy of one per cent in \bar{b} , as a substitution of calculated results for b_1 etc. into (4.20) would show.

(iv) Calculation of entrainment velocity.

From the continuity equation (4.1) the following relations for entrainment velocity is obtained

$$\bar{V} = \frac{1}{\bar{\rho}r} \int_0^r \frac{\partial}{\partial r} (\bar{\rho} \bar{V} r) dr = - \frac{1}{\bar{\rho}r} \int_0^r \frac{\partial}{\partial x} (\bar{\rho} \bar{u} r) dr \quad (4.29)$$

$$\text{Now } \left(\frac{\partial}{\partial x}\right)_r = \left(\frac{\partial \xi}{\partial x}\right)_r \left(\frac{\partial}{\partial \xi}\right)_\zeta + \left(\frac{\partial \zeta}{\partial x}\right)_r \left(\frac{\partial}{\partial \zeta}\right)_\xi = \frac{\kappa}{r_0} \left(\frac{\partial}{\partial \xi}\right)_\zeta - \frac{\kappa}{r_0 \hat{b}} \left(\zeta \frac{d\hat{b}}{d\xi} + \frac{d\hat{r}_1}{d\xi}\right) \left(\frac{\partial}{\partial \zeta}\right)_\xi \quad (4.30)$$

Therefore eqn. (4.29) leads to the following equation for entrainment velocity

$$r_0 \frac{V_\infty}{\kappa} = -\frac{1}{\bar{\rho}_\infty r_2} \int_0^{r_2} \frac{\partial}{\partial \xi} (\bar{\rho} \bar{u} r) dr + \frac{1}{\bar{\rho}_\infty r_2} \int_0^{r_2} \left\{ \frac{\zeta}{\hat{b}} \frac{d\hat{b}}{d\xi} + \frac{1}{\hat{b}} \frac{d\hat{r}_1}{d\xi} \right\} \frac{\partial (\bar{\rho} \bar{u} r)}{\partial \zeta} dr$$

but \bar{u} has been assumed to be a function of ζ only, thus the first term on the right-hand side is zero. Changing integration variables from r to ζ leads to

$$\frac{V_\infty}{\kappa u_J}$$

$$\begin{aligned} \frac{V_\infty}{\kappa u_J} = & \frac{\hat{b}\lambda_T}{\hat{r}_2} \left\{ \frac{d\hat{b}}{d\xi} \int_0^1 \frac{d}{d\zeta} (\zeta RU) \zeta d\zeta + \frac{\hat{r}_1}{\hat{b}} \frac{d\hat{b}}{d\xi} \int_0^1 \frac{d}{d\zeta} (RU) \zeta d\zeta \right. \\ & \left. + \frac{d\hat{r}_1}{d\xi} \int_0^1 \frac{d}{d\zeta} (RU\zeta) d\zeta + \frac{\hat{r}_1}{\hat{b}} \frac{d\hat{r}_1}{d\xi} \int_0^1 \frac{d}{d\zeta} (RU) d\zeta \right\} \end{aligned} \quad (4.31)$$

where $\lambda_T = T_\infty/T_J$.

Further simplification can be obtained by integrating by parts the integrals in eqn. (4.31), thereby after some rearrangement the final form given below for the entrainment velocity is obtained.

$$\begin{aligned} (\hat{r}_1 + \hat{b})V_\infty/(\kappa u_J) = & \hat{b}(d\hat{b}/d\xi) \{ \lambda - \lambda_T + \lambda_T \Delta_3 \} + \hat{b}(d\hat{r}_1/d\xi)\lambda \\ & + \hat{r}_1(d\hat{b}/d\xi) \{ \lambda - \lambda_T + \lambda_T \Delta_1 \} + \hat{r}_1(d\hat{r}_1/d\xi)(\lambda - \lambda_T) \end{aligned} \quad (4.32)$$

$$\text{where } \Delta_3 = \int_0^1 (1 - RU\zeta) d\zeta \quad (4.33)$$

In the limit as $\xi \rightarrow 0 (\hat{b} \rightarrow 0)$ eqn. (4.32) becomes

$$V_\infty/(\kappa u_J) = b_1 \{ (\lambda - \lambda_T)\eta_2 + \lambda_T \Delta_1 \} \quad (4.34)$$

This is equivalent to the two-dimensional result. Obviously, it is the mass-entrainment rate per unit length, $2\pi\rho_\infty rV_\infty$, which must tend to a constant as $r \rightarrow \infty$ in an axisymmetric jet, so when comparing it to the two-dimensional case r_2V_∞ should be used rather than V_∞ .

(v) Calculation of the dividing streamline.

The dividing streamline is defined as the one which divides the fluid originally in the jet from the fluid entrained from the surroundings. This means that the mass flux below the dividing streamline remains unchanged, i.e.

$$\pi r_0^2 \rho_J u_J = 2\pi \int_0^{r_d} \bar{\rho} \bar{u} r dr \quad (4.35)$$

or, after substitution and rearrangement

$$1 - \hat{r}_1^2 = 2\hat{b}^2 \int_0^{\zeta_d} RU\zeta d\zeta + 2\hat{b}\hat{r}_1 \int_0^{\zeta_d} RU d\zeta \quad (4.36)$$

Eqn. (4.36) is an implicit equation for ζ_d and must be solved numerically.

In the limit $\xi \rightarrow 0 (\hat{b} \rightarrow 0)$ eqn. (4.36) reduces to

$$\eta_1 = (1 - \hat{r}_1)/\hat{b} = \int_0^{\zeta_d} RU d\zeta \quad (4.37)$$

which is, of course, equivalent to the result for the two-dimensional mixing layer.

5. Discussion of results.

(i) Comparison with other experimental and theoretical results.

Although the analysis presented in Section 4 is valid for the case where $u_\infty \neq 0$, results have only been calculated for $u_\infty = 0$. However, approximate analytical formulae for b_1 , Δ_1 and Δ_2 are given in Appendix I whereby most of the quantities of interest can be determined for the case of $u_\infty \neq 0$.

Calculated values of b_1 , b_2 , b_3 , b_4 , I_B and J_B are given in Table I for a comprehensive range of Mach numbers and stagnation enthalpy ratios. Similarly, Δ_1 , Δ_2 and Δ_3 are listed in Table II. Almost all properties of practical interest may be evaluated using these tables in conjunction with the equations given in Section 4.

Selected properties are also presented graphically. The boundaries, \hat{r}_1 and \hat{r}_2 , and dividing-streamline position for a low speed axisymmetric heated mixing layer are presented in Fig. 2 for a comprehensive range of temperature ratios. The development of entrainment and dividing-streamline velocities for the same are plotted in Figs. 3 and 4 respectively. Fig. 7 presents curves showing the variation of potential-core length with Mach number and stagnation-enthalpy ratio. The remaining figures display plots of two-dimensional properties for a comprehensive range of Mach number and stagnation-enthalpy ratio.

A useful source of comparative data is the series of papers written by Szablewski on low speed mixing layers with $T_J \neq T_\infty$. The results for spreading rate and entrainment velocity, shown in Figs. 5 and 8 respectively, compare fairly favourably with his. Szablewski's values for b_1 and $-\{V_\infty / (\kappa u_J)\}_{\zeta=0}$ were estimated using his values for the spreading parameter, σ , [where $\sigma = (2\kappa b_1)^{-1}$]. Since he assumed that $Pr_T = 0.5$ it may be inferred that the spreading rate and entrainment velocity are not too sensitive to the value of Pr_T .

A direct comparison of the η_2 predictions in Fig. 6 was only possible for Szablewski (1957). Values of η_2 could be estimated approximately from velocity profiles given elsewhere, but this procedure leads to such rough results as not to be worthwhile. Since the present velocity profiles are only approximations, it could not be expected that the predictions for η_2 , η_d and \bar{U}_d/u_J in Figs. 6, 9 and 10 respectively would be very accurate. The value of \bar{U}_d/u_J seems to be especially sensitive to the precise shape of the velocity profile. A comparison between the present predictions and some previous theoretical results is presented in Fig. 12. It can be seen that the present results lie slightly above those of Korst et al (1954) who used the error-function profile. In addition, it will be noted, from a comparison of the accurate results of Jacques and Gailly (1966) and Carpenter and Tabakoff (1971), that the value of Pr_T has quite a noticeable effect at the higher values of Mach number. Although the results plotted in Fig. 10 are not very accurate in absolute value, they probably indicate

the effect of a change in M_J and λ_H quite adequately. In any case if \bar{u}_d/u_J is so sensitive to the precise velocity-profile shape, it is unlikely that in practice the value could be predicted within 10% accuracy.

It is evident from Fig. 7 that when $T_J < T_\infty$ there is a considerable divergence between the present estimate for the potential-core length and Szablewski's (1963) result. His prediction for $\hat{r}_1(x)$ shows the inner edge turning very abruptly towards the axis near the end of the potential core. This effect is absent in Fig. 2 and in Szablewski (1961) where $T_J > T_\infty$. The reasons for this discrepancy are not apparent. In addition to Szablewski's theoretical results, Bezmenov and Borisov's experimental value of $1/\xi_{pc}$ for a very hot jet is plotted in Fig. 7. This value comes from Fig. 13 of Golubev (1967) who gives $x_{pc}/r_o = 5$ for $T_J/T_\infty = 15$ compared to $x_{pc}/r_o = 8$ for $T_J/T_\infty = 1$. It can be seen that this experimental point agrees very well with the theoretical curve. A data point from Balashov (1958) is also included in Fig. 7, x_{pc} was taken as $11.5 r_o$ in this case. Finally, data points from Corrsin and Uberoi (1950) are also included on Fig. 7.

The agreement between the theoretical curve for $1/\xi_{pc}$ in Fig. 7 and the experimental data for strongly heated mixing layers is good enough to suggest that the inverse turbulent Reynolds number, κ , is invariant with stagnation-enthalpy ratio. In addition, Szablewski (1958) compared his results for a hot jet in a moving stream to the experimental data of Pabst (1960) ($u_\infty/u_J = 0.47$ and 0.06 , $T_\infty/T_J \approx 0.43$), and concluded that κ remains unchanged. Since Szablewski's results agree very well with the present ones, this can be regarded as further evidence corroborating the conclusion that κ does not vary with temperature ratio.

It is immediately apparent from Fig. 11 that the existence of a considerable scatter in the data taken from various sources constitutes a major difficulty in comparing predicted spreading rates with experimental ones. Even at $M_J = 0$ there is a 25 per cent difference between Wagnanski and Fiedler's (1970) value of κ and Liepmann and Laufer's (1947) value. This scatter can probably be partly explained by the sensitivity of turbulent mixing layers to their initial conditions. This was brought out by the experiments reported in Bradshaw (1966) who showed that a mixing layer developing from a fully turbulent boundary layer tends to a higher level of turbulence (i.e. larger κ) than one in which transition occurs after separation. This effect has been confirmed by Jones (1969). It happens that Wagnanski and Fiedler had fully turbulent initial conditions while with Liepmann and Laufer transition occurs after separation.

Another effect, possibly connected with the preceding one, is reported by Crow and Champagne (1971). They show, inter alia, that a mixing layer subjected to pressure fluctuations of certain frequencies spreads at a greater rate. This observation is also corroborated by Kel'manson's (1968) experiments. Thus the possibility exists that acoustic radiation, originating in the mixing layer, can be reflected back into it by adjacent surfaces, causing a modification to the mixing properties. A similar phenomenon was certainly observed by Glass (1968)

in compressible jets. He found that if the reflecting surfaces were adjusted to maximise the effect of acoustic feedback then a 50 per cent increase in spreading rate could be achieved. This effect could be responsible for the large difference between Johannesen's (1962) values for σ , obtained in a jet with internal shock waves. The first shock cell yielded $\sigma = 21.9$ followed by an abrupt change to 11.9 after interaction with a weak shock wave.

Recently Birch and Eggers (1972) have critically examined the experimental data for spreading parameter. They suggested that many of the investigations have been carried out on mixing layers which were not really fully developed. Their recommended variation of σ with Mach number is shown in Fig. 11, a comparison of this variation with the theoretical predictions for b_1 leads to the following variation of κ with Mach number:

TABLE III

M_J	κ/κ_0
0	1.0
1.0	1.0
1.5	0.86
2.0	0.68
3.0	0.51
4.0	0.47
5.0	0.46

The predicted entrainment velocity agrees exactly with Liepmann and Laufer's measured value of $\kappa = 0.0055$. Using this value, appropriately modified using Table III, Johannesen's (1963) experimental value for entrainment velocity is plotted in Fig. 8. The agreement with the theoretical curve is excellent. Johannesen's value for entrainment velocity was deduced from his Figure 23 which gave a value of $2\pi r_2 \rho_\infty V_\infty$; r_2 was taken as equal to r_0 since the measuring point was near the nozzle exit. Hill & Nicholson's (1964) experimental data were all predicted to within 10% accuracy by the following semi-empirical formulae

$$\frac{V_\infty}{u_J} = 0.049 \left(\frac{\rho_\infty}{\rho_J}\right)^{-0.6} \left(1 + \frac{\gamma-1}{2} M_J^2\right)^{-0.67}$$

This formula will only agree with Liepmann & Laufer's result if the constant is changed to 0.033. Therefore, acting on the premise that Hill & Nicholson's mixing layers had unusually high spreading rates, their actual measured values are reduced by a factor of 0.033/0.049 when plotted in Fig. 8. In spite of this adjustment the experimental values are still about 30% larger than the theoretical predictions, although the variation with total-enthalpy ratio appears to be correctly predicted.

(ii) Physical interpretation of theoretical formulae and results.

V_∞ , η_2 , and db/dx can be regarded as being determined respectively from a mass, momentum and energy balance applied to an elemental slice of mixing layer. To appreciate this consider a slice near the origin in Fig. 1 of width dx , where the mixing layer may be treated as two-dimensional.

A mass balance gives

$$\frac{db}{dx} \int_0^1 RU d\eta = \eta_1 \frac{db}{dx} + \frac{\lambda}{\lambda_T} \eta_2 \frac{db}{dx} - \frac{V_\infty}{\lambda_T u_J} \quad (5.1)$$

while a momentum balance gives

$$\frac{db}{dx} \int_0^1 RU^2 d\eta = \eta_1 \frac{db}{dx} + \frac{\lambda^2}{\lambda_T} \eta_2 \frac{db}{dx} - \frac{\lambda}{\lambda_T} \frac{V_\infty}{u_J} \quad (5.2)$$

and an energy balance gives

$$\frac{db}{dx} \int_0^1 RU^3 d\eta = \eta_1 \frac{db}{dx} + \frac{\lambda^3}{\lambda_T} \eta_2 \frac{db}{dx} - \frac{\lambda^2}{\lambda_T} \frac{V_\infty}{u_J} - 2\kappa(1-\lambda) \int_0^1 R \left(\frac{dU}{d\eta} \right)^2 d\eta \quad (5.3)$$

The last term on the right-hand side of eqn. (5.3) represents the dissipation of mean-flow kinetic energy by the turbulence. It takes this particular form because the rate at which mean-flow energy is lost to the turbulence is given by

$$-\rho \overline{u'v'} \frac{\partial \bar{u}}{\partial y} = \bar{\rho} (u_J - u_\infty) b \left\{ \frac{\partial \bar{u}}{\partial y} \right\}^2$$

When $u_\infty = 0$ (i.e. $\lambda=0$) V_∞/u_J , η_2 and db/dx may be determined directly from the three equations given above (N.B. $\eta_2 + \eta_1 = 1$). However, when $\lambda \neq 0$ it is necessary to eliminate V_∞/u_J from (5.2) and (5.3) to obtain eqns. (4.23) and (4.25).

Henceforth only the ($u_\infty = 0$) case will be considered.

The limiting forms of R as $\lambda_H \rightarrow 0$ and ∞ , help to explain the effect of strong heating on the mixing-layer properties. From eqn. (4.7) it follows that

$$R \rightarrow \frac{1}{U\{(1+m) - mU\}} \text{ as } \lambda_H \rightarrow 0 \text{ and } R \rightarrow \frac{1}{\lambda_T(1-U)} \text{ as } \lambda_H \rightarrow \infty \quad (5.4)$$

As the jet is heated to an increasingly high temperature, the surrounding air will have a relatively greater density. Therefore the small change in velocity, occurring as one moves inward from the outer edge, leads to a relatively large change in momentum flux. This results in the mixing layer being deflected towards the jet axis (i.e. η_2 becomes smaller). A rise in Mach number enhances the effect because this causes the gas in the jet to become even more rarified. On the other hand when the surrounding air is heated ($\lambda_H > 1$) the effect is

reversed and η_2 rises. Ultimately when $\lambda_H \rightarrow \infty$ then $\eta_2 \rightarrow 1$ as is evident from eqn. (5.4) and (5.2). The influence of a change in M_J is much less pronounced for the ($\lambda_H > 1$) case. These qualitative arguments are borne out by the results presented in Fig. 6.

Why do turbulent mixing layers spread? They spread because momentum and energy are convected laterally by means of the turbulent fluctuations. Also, because mean-flow energy is converted into turbulence energy. To paraphrase eqn. (5.3) in words

{The spreading rate}

$$= \left\{ \begin{array}{l} \text{(Rate at which kinetic energy enters the mixing layer from the jet core)} \\ - \text{(Rate at which it crosses a section of the mixing layer)} \end{array} \right\} \\ \div \left\{ \begin{array}{l} \text{Rate at which mean-flow kinetic energy is converted into turbulence} \\ \text{energy} \end{array} \right\} \quad (5.5)$$

As the jet-core becomes hotter, η_2 diminishes. Thus the rate at which energy enters the mixing layer rises in relative terms, increasing the numerator in eqn. (5.5). On the other hand the Reynolds shear stress is reduced because of the considerable reduction in density over much of the mixing layer. Thus the denominator in eqn. (5.5) falls. Hence the spreading rate rises as the jet becomes hotter. Since an increase in M_J means a reduction in ρ_J , the spreading rate also rises with M_J . These arguments can be reversed if the surrounding air is heated ($\lambda_H > 1$); except that in the limit $\lambda_H \rightarrow \infty$, db/dx becomes independent of M_J , because for finite M_J the core density ρ_J is always infinitely greater than ρ_∞ (c.f. eqn. 5.4). These arguments are corroborated by Fig. 5.

An entrainment coefficient, c_q , is defined as

$$c_q = - \frac{\rho_\infty V_\infty}{\rho_J u_J} = - \frac{V_\infty}{\lambda_T u_J} \quad (5.6)$$

This represents the mass entrainment per unit surface area. It is clear from eqn. (5.1) that

$$c_q = \left(\begin{array}{l} \text{Rate of change in mass flux at a section} \\ - \text{Rate at which mass enters per unit area of mixing layer from jet core} \end{array} \right) \quad (5.7)$$

Now c_q rises with T_J for two reasons:

- (i) db/dx becomes larger, thereby augmenting both terms in eqn. (5.7);
- (ii) the reduction in ρ_J increases their difference owing to the outer part of the mixing layer tending to make a bigger contribution to the first term,

Consequently/

Consequently, c_q rises in value as the jet becomes hotter and decreases when the secondary air becomes hotter. This can be clearly seen in Fig. 8. However, $-V_\infty/u_J = c_q \lambda_T$, so as the jet core gets increasingly hot, a smaller and smaller entrainment velocity is required to make up the required value of c_q , and vice-versa when $\lambda_H > 1$. Ultimately when $\lambda_H \rightarrow 0$ it can be seen from eqns, (5,1) and (5,4) that $V_\infty \rightarrow 0$; whereas when $\lambda_H \rightarrow \infty$

$$-\frac{V_\infty}{u_J} \rightarrow \frac{db}{dx} \int_0^1 U dn \quad (5,8)$$

Fig. 8 confirms this.

If M_J is fixed then u_J varies as $\sqrt{T_{0J}}$. Therefore the value of V_∞ relative to its unheated value can be obtained by dividing V_∞/u_J by $\lambda_H^{1/2}$. As Fig. 8 shows, this quantity remains almost invariant over the practical range of λ_H for hot jets.

Finally, the ratio of c_q to its unheated value serves as a measure of the mixing layer's "efficiency" as a mass-entrainment mechanism. This quantity {multiplied by $(c_q)_{\lambda_H=1}$ } is also plotted in Fig. 8 for $M_J = 0$. It is apparent that ($\lambda_H < 1$) mixing layers are relatively very "efficient", e.g. the $\lambda_H = 0,2$ case is two and half times more "efficient" than when $\lambda_H = 1$.

The behaviour of the dividing streamline with change in λ_H and M_J is easy to understand. η_d depends on the rate at which mass enters the mixing layer from the jet core, in other words it depends on η_2 . This is obvious from eqn. (4,35). Hence η_d rises and u_d falls when the jet is heated and vice-versa when $\lambda_H > 1$. A rise in Mach number has a similar effect to heating. It follows from eqns, (4,35) and (5,4) that $\lim_{\lambda_H \rightarrow \infty} \{\eta_d \text{ and } u_d\}$ is independent of M_J . These prognostications

are given quantitative dimensions in Figs. 9 and 10.

The effects of axial symmetry have not been discussed. They are almost entirely what would have been expected. Therefore Figs. 2, 3 and 4 are left to speak for themselves.

6. Conclusions

(i) The variations of such properties as spreading rate, the position of the inner and outer edges and entrainment velocity, are determined for an axisymmetric mixing layer. Comprehensive ranges of Mach number and stagnation-enthalpy ratio are taken.

(ii) A comparison between the predicted properties and available experimental data corroborates the premise that the constant in the Prandtl-Görtler eddy-viscosity model is invariant with respect to changes in temperature for low speeds. A recommended variation of κ with Mach number is given in Table III (p.12).

(iii) The non-dimensional entrainment velocity, $V_{\infty}/(\kappa u_J)$, is found to be almost invariant with change in Mach number. For a fixed Mach number, $V_{\infty}/(V_{\infty})_{\lambda_H=1}$ is found to vary only slightly for $0.2 \leq \lambda_H \leq 1.0$. The mixing layer in a hot jet is found to be a much more efficient mechanism for mass entrainment than its unheated equivalent.

(iv) The cool jet issuing into a hot medium is shown to have a mixing layer with properties which are invariant with changes in Mach number for the limit $T_{\infty}/T_J \rightarrow \infty$.

(v) The entrainment velocity of a two-dimensional mixing layer is not directly proportional to the spreading rate when the Mach number and total-enthalpy ratio is varied. This is clearly shown by eqn. (4.34).

Acknowledgements

The author was supported by Rolls-Royce (1971) Limited as a Research Fellow while engaged on the research described above. He would also like to thank Professor N.H. Johannesen for his help and guidance.

References

- Abramovich, G.N. 1963 "The theory of turbulent jets", MIT Press
- Alpinieri, L.J. 1964 "Turbulent mixing of coaxial jets", AIAA J. 2, 1560
- Balashov, G.V. 1958 "Turbulent jets issuing into surroundings at high temperature" (in Russian), Rostovskii Institut Inzhenerov Zheleznodorozhnogo Transporta, Vypusk 21, Voprosy konstruktsii i teorii lokomotivov, pp 156-169
- Bershader, D. and S.I. Pai 1950 "On turbulent jet mixing in two-dimensional supersonic flow", J. Appl. Phys. 21, 616
- Birch, S.F. and J.M. Eggers 1972 "A critical review of the experimental data for developed free turbulent shear layers", NASA SP-321, Vol.1, 11
- Bradshaw, P. 1966 "The effect of initial conditions on the development of a free shear layer", JFM 26, 225
- Bradshaw, P. 1967 "The insensitivity of turbulent flows to changes in Reynolds number and Mach number", NPL Aero. Note 1057
- Bradshaw, P., D.H. Ferris and N.P. Atwell 1967 "Calculation of boundary-layer development using the turbulent energy equation", JFM 28, 593
- Bradshaw, P. and D.H. Ferris 1971 "Calculation of boundary-layer development using the turbulent energy equation: compressible flow on adiabatic walls", JFM 46, 83
- Broer, L.J.F. and J.A. Rietdijk 1960 "Measurements on supersonic free jets", Appl. Sci. Res. A9, 465
- Carpenter, P. and W. Tabakoff 1971 "The initial development of the general non-isoenergetic compressible free shear layer", NASA CR-1828
- Channapragada, R.S. 1963 "Compressible jet spread parameter for mixing zone analysis", AIAA J. 1, 2188
- Channapragada, R.S. and J.P. Wooley 1967 "Turbulent mixing of parallel compressible non-isoenergetic streams", Astro. Acta 13, 341
- Chapman, D.R. 1950 "An analysis of base pressure at supersonic velocities and comparison with experiment", NACA TN 2137

- Chrisman, C.C. 1962 "Evaluation of the free jet spreading rate parameter for axisymmetric flow of air at Mach number 3.0", M.S. Thesis, Oklahoma State University.
- Cook, E.B. and J.M. Singer 1969 "Predicted air entrainment by subsonic free round jets", J. Spacecraft & Rockets 6, 1066
- Corrsin, S. and M.S. Uberoi 1950 "Further experiments on the flow and heat transfer in a heated turbulent jet of air", NACA Rep. 998 (replaces NACA TN 1865)
- Crane, L.J. 1957 "The laminar and turbulent mixing of jets of compressible fluid, II The mixing of two semi-infinite streams", JFM 3, 81
- Crow, S.C. and F.H. Champagne 1971 "Orderly structure in jet turbulence", JFM 48, 547
- Demetriades, A. and E.L. Doughman 1969 "Mean and intermittent flow of a self-preserving plasma jet", AIAA J. 7, 713
- Donaldson, C. du P. and K.E. Gray 1966 "Theoretical and experimental investigation of the compressible free mixing of two dissimilar gases", AIAA J. 4, 2017
- Ferri, A, P.A. Libby and V. Zakkay 1962 "Theoretical and experimental investigation of supersonic combustion", PIBAL Rep. No. 713
- Glass, D.R. 1968 "Effects of acoustic feedback on the spread and decay of supersonic jets", AIAA J. 6, 1890
- Golubev, V.A. 1967 "High-temperature jets", in Turbulent jets of air, plasma and real gases (G.N. Abramovich, Ed.), Trans. and Pub. by Consultants Bureau, N.Y. 1969
- Gooderum, P.B., G.P. Wood and M.J. Brevort 1949 "Investigation with an interferometer of the turbulent mixing of a free supersonic jet", NACA TN 1857
- Görtler, H. 1942 "Berechnung von Aufgaben der freien Turbulenz auf Grund eines neuen Näherungsansatzes", ZAMM 22, 244
- Herring, H.J. and G.L. Mellor 1968 "A method of calculating compressible turbulent boundary layers", NASA CR-1144
- Hill, J.A.F. and J.E. Nicholson 1964 "Compressibility effect on fluid entrainment in turbulent mixing layers", NASA CR-131
- Hill, W.G. 1966 "Initial development of compressible turbulent free shear layers", Ph.D. thesis, Rutgers - The State University

- Hinze, J.O. and B.G. van der H. Zijnen 1949 "Transfer of heat and matter in the turbulent mixing zone of an axially symmetric jet", App. Sci. Res. 1, 435
- Jacques, R. and A. Gailly 1966 "Melange supersonique turbulent et application aux problemes de recollement", AGARD Conf. Proc. No.4
- Johannesen, N.H. 1957 "The mixing of free axially symmetrical jets of Mach number 1.40", ARC R & M 3291
- Johannesen, N.H. 1959 "Further results on the mixing of free axially symmetrical jets of Mach number 1.40", ARC R & M 3292
- Jones, I.S.F. 1969 "Fluctuating turbulent stresses in the noise producing region of a jet", JFM 36, 529
- Kel'manson, I.A. 1968 "Some data on the structure of turbulent jets", (in Russian) KazSSR Gylym Akad. Khabarshysy, Vestn. Akad. Nauk KazSSR No. 3, 51-58
- Kleinstein, G. 1964 "Mixing in turbulent axially symmetric free jets", J. Spacecraft & Rockets 1, 403
- Korst, H.H. 1956 "A theory for base pressures in transonic and supersonic flow", J. Appl. Mech. 23, 593
- Korst, H.H. and W.L. Chow 1966 "Non-isoenergetic turbulent ($Pr_T=1$) jet mixing between two compressible streams at constant pressure", NASA CR-419
- Korst, H.H., R.H. Page and M.E. Childs 1954 "Compressible two-dimensional jet mixing at constant pressure", Univ. of Illinois, ME TN 392-1
- Laufer, J. 1969 "Turbulent shear flows of variable density", AIAA J. 7, 706
- Libby, P.A. 1962 "Theoretical analysis of turbulent mixing of reactive gases with application to supersonic combustion of hydrogen", ARS J. 32, 388
- Liepmann, H.W. and J. Laufer 1947 "Investigation of free turbulent mixing", NACA TN 1257
- Maise, G. and H. McDonald 1968 "Mixing length and kinematic eddy viscosity in a compressible boundary layer", AIAA J. 6, 73
- Maydew, R.C. and J.F. Reed 1963 "Turbulent mixing of compressible free jets", AIAA J. 1, 1443

- Mills, R.D. 1968 "Numerical and experimental investigation of the shear layer between two parallel streams", JFM 33, 591
- Morkovin, M. 1962 "Effects of compressibility on turbulent flows", in The Mechanics of Turbulence (A. Favre, Ed.) Gordon and Breach Sci. Publ. Inc. pp 367-380
- Pabst, O. 1960 "Die Ausbreitung heisser Gasstrahlen in bewegter Luft", Luftfahrttechnik 6, 271
- Pai, S.I. 1949 "Two-dimensional jet mixing of a compressible fluid", J. Aero. Sci. 16, 463
- Pai, S.I. and B.B. Cary 1955 "Two-dimensional jet mixing of supersonic flow", 50 Jahre Grenzschichtforschung (H. Görtler and W. Tollmien, Eds.) Friedr. Vieweg & Sohn, Braunschweig
- Prandtl, L. 1942 "Bemerkung zur Theorie der freien Turbulenz", ZAMM 22, 241
- Schetz, J.A. 1968 "Turbulent mixing of a jet in a coflowing stream, AIAA J. 6, 2008
- Sirieux, M. and J.L. Solignac 1966 "Contribution à l'étude expérimentale de la couche de mélange turbulent isobare d'un écoulement supersonique", AGARD CP No. 4, 241
- Smoot, L.D. and W.E. Purcell 1967 "Model for mixing of a compressible free jet with a moving environment", AIAA J. 5, 2049
- Szablewski, W. 1957 "Turbulente Vermischung ebener Heissluftstrahlen", Ing.-Arch. 25, 10
- Szablewski, W. 1958 "Turbulente Ausbreitung runder Heissluftstrahlen in bewegter Luft (Erster Teil: Kerubereich)", Ing.-Arch. 26, 358
- Szablewski, W. 1961 "Turbulente Ausbreitung eines runden Heissluftstrahls in ruhender Aussenluft - Erster Teil: Kernbereich", Ing.-Arch. 30, 96
- Szablewski, W. 1963 "Turbulente Vermischung runder Kaltluftstrahlen mit umgebender ruhender Heissluft", Int. J. Heat Mass Transfer 6, 739
- Ting, L. and P.A. Libby 1960 "Remarks on the eddy viscosity in compressible mixing flows", J. Aero. Sci. 27, 797
- Tufts, L.W. and L.D. Smoot 1971 "A turbulent mixing coefficient correlation for coaxial jets with and without secondary flows", J Spacecraft and Rockets 8, 1183

- Warren, W.R. 1957 "An analytical and experimental study of compressible free jets", Princeton Univ. Dept. Aero. Eng. Rep. 381
- Wynanski, I. and H.E. Fiedler 1970 "The two-dimensional mixing region", JFM 41, 327
- Zumwalt, G.W. 1959 "Analytical and experimental study of the axially-symmetric supersonic base pressure problem", Ph.D. Thesis Univ. of Illinois.

TABLE I

THE VALUES OF CERTAIN PARAMETERS INVOLVED IN CALCULATIONS OF
THE CHARACTERISTICS OF AN AXISYMMETRIC TURBULENT MIXING LAYER

$\frac{1-\lambda_H}{1+\lambda_H}$	b_1	b_2	b_3	b_4	I_B	J_B
-----------------------------------	-------	-------	-------	-------	-------	-------

$M_J = 0$

-1.0	23.00	-14.5	108	-930	0	0
-0.8	38.21	31.6	327	-90	0.0410	0.2415
-0.6	44.76	64.8	609	2262	0.0585	0.3043
-0.4	49.58	94.1	934	5694	0.0708	0.3423
-0.2	53.67	122.0	1307	10280	0.0809	0.3704
0	57.42	149.7	1742	16270	0.0898	0.3934
0.2	61.09	178.2	2261	24160	0.0982	0.4136
0.4	64.90	208.9	2906	34820	0.1065	0.4324
0.6	69.13	243.5	3764	50070	0.1154	0.4511
0.8	74.45	286.0	5063	74470	0.1258	0.4713
1.0	84.46	352.1	8266	131200	0.1431	0.5000

$M_J = 1$

-1.0	23.00	-14.5	108	-930	0	0
-0.8	36.88	25.3	289	-386	0.0371	0.2257
-0.6	43.15	54.6	523	1358	0.0537	0.2881
-0.4	47.81	80.7	796	3955	0.0655	0.3261
-0.2	51.78	105.5	1112	7458	0.0752	0.3542
0	55.45	130.2	1481	12060	0.0838	0.3771
0.2	59.05	155.6	1923	18130	0.0918	0.3972
0.4	62.79	182.9	2476	26320	0.0997	0.4158
0.6	66.96	213.5	3212	37980	0.1081	0.4341
0.8	72.19	250.7	4329	56390	0.1178	0.4537
1.0	82.00	306.7	7078	96610	0.1336	0.4806

$M_J = 2$

-1.0	23.00	-14.5	108	-930	0	0
-0.8	34.18	14.0	226.7	-800	0.0293	0.1911
-0.6	39.80	35.9	383.0	33	0.0439	0.2521
-0.4	44.08	55.6	567.8	1355	0.0545	0.2899
-0.2	47.79	74.4	784.2	3185	0.0632	0.3178

TABLE I (Contd)

0	51,24	93,2	1040	5618	0,0709	0,3406
0.2	54,66	112,5	1351	8835	0,0782	0,3603
0.4	58,23	133,1	1741	13150	0,0852	0,3784
0.6	62,23	155,8	2266	19180	0,0926	0,3959
0.8	67,26	182,6	3069	28250	0,1010	0,4141
1.0	76,57	220,1	5051	44170	0,1137	0,4374

$M_J = 3$

-1,0	23,00	-14,5	108	-930	0	0
-0.8	31,66	5,0	184	-1013	0,0221	0,1552
-0.6	36,55	20,5	286	-724	0,0344	0,2135
-0.4	40,40	34,6	408	-183	0,0436	0,2504
-0.2	43,78	48,2	553	604	0,0513	0,2778
0	46,98	61,8	726	1668	0,0581	0,3002
0.2	50,17	75,5	938	3072	0,0644	0,3195
0.4	53,53	90,1	1209	4918	0,0706	0,3370
0.6	57,31	105,8	1577	7363	0,0770	0,3537
0.8	62,07	123,6	2147	10600	0,0840	0,3705
1.0	70,82	146,4	3574	12510	0,0940	0,3906

$M_J = 4$

-1,0	23,00	-14,50	108	-930	0	0
-0.8	29,72	-10,11	160	-1095	0,0166	0,1248
-0.6	33,96	10,06	231	-1066	0,0269	0,1792
-0.4	37,39	20,24	315	-916	0,0348	0,2146
-0.2	40,46	30,03	417	-659	0,0415	0,2413
0	43,41	39,71	540	-298	0,0475	0,2631
0.2	46,37	49,50	693	170	0,0530	0,2819
0.4	49,51	59,60	890	737	0,0584	0,2988
0.6	53,08	70,24	1163	1339	0,0639	0,3147
0.8	57,57	81,69	1592	1626	0,0698	0,3303
1.0	65,80	94,82	2678	-2831	0,0778	0,3481

Contd/

TABLE I (Contd)

-1.0	23,00	-14,5	108	-930	0	0
-0.8	28,31	-4,90	147	-1119	0,0127	0,1007
-0.6	31,98	3,17	198	-1213	0,0213	0,1506
-0.4	35,05	10,62	262	-1254	0,0281	0,1842
-0.2	37,85	17,75	338	-1263	0,0339	0,2098
0	40,56	24,74	432	-1258	0,0391	0,2309
0.2	43,31	31,72	549	-1267	0,0440	0,2491
0.4	46,26	38,76	702	-1351	0,0487	0,2653
0.6	49,62	45,90	917	-1679	0,0535	0,2805
0.8	53,87	53,05	1259	-2842	0,0586	0,2952
1.0	61,65	59,94	2136	-10050	0,0651	0,3113

TABLE II
THE VALUES OF CERTAIN INTEGRAL PROPERTIES IN
AN AXISYMMETRIC TURBULENT MIXING LAYER

$\frac{1-\lambda_H}{1+\lambda_H}$	$M_J=0$			$M_J=1$		
	Δ_1	Δ_2	Δ_3	Δ_1	Δ_2	Δ_3
-1.0	1.0000	1.0000	1.0000	1.0000	1.0000	1.0000
-0.8	0.7297	0.7585	0.9477	0.7492	0.7743	0.9532
-0.6	0.6468	0.6957	0.9203	0.6689	0.7119	0.9280
-0.4	0.5901	0.6577	0.8982	0.6143	0.6739	0.9076
-0.2	0.5432	0.6296	0.8776	0.5694	0.6458	0.8888
0	0.5000	0.6066	0.8569	0.5286	0.6229	0.8699
0.2	0.4568	0.5864	0.8344	0.4881	0.6028	0.8496
0.4	0.4099	0.5676	0.8080	0.4448	0.5842	0.8260
0.6	0.3532	0.5489	0.7735	0.3932	0.5659	0.7955
0.8	0.2703	0.5287	0.7179	0.3192	0.5463	0.7469
1.0	0	0.5000	0.5000	0.0866	0.5194	0.5611
	$M_J=2$			$M_J=3$		
-1.0	1.0000	1.0000	1.0000	1.0000	1.0000	1.0000
-0.8	0.7905	0.8089	0.9639	0.8317	0.8448	0.9733
-0.6	0.7157	0.7479	0.9431	0.7634	0.7865	0.9567
-0.4	0.6653	0.7101	0.9262	0.7171	0.7496	0.9431
-0.2	0.6246	0.6822	0.9108	0.6802	0.7222	0.9306
0	0.5881	0.6594	0.8955	0.6478	0.6998	0.9185
0.2	0.5530	0.6397	0.8793	0.6172	0.6805	0.9058
0.4	0.5164	0.6216	0.8608	0.5863	0.6630	0.8917
0.6	0.4743	0.6041	0.8375	0.5521	0.6463	0.8743
0.8	0.4166	0.5859	0.8015	0.5077	0.6295	0.8485
1.0	0.2500	0.5626	0.6717	0.3918	0.6094	0.7610

Contd/

TABLE II (Contd)

$\frac{1-\lambda_H}{1+\lambda_H}$	$M_J=4$			$M_J=5$		
	Δ_1	Δ_2	Δ_3	Δ_1	Δ_2	Δ_3
-1.0	1.0000	1.0000	1.0000	1.0000	1.0000	1.0000
-0.8	0.8658	0.8752	0.9802	0.8923	0.8993	0.9850
-0.6	0.8039	0.8208	0.9669	0.8367	0.8494	0.9742
-0.4	0.7614	0.7854	0.9558	0.7977	0.8158	0.9651
-0.2	0.7276	0.7587	0.9457	0.7665	0.7902	0.9567
0	0.6983	0.7669	0.9359	0.7396	0.7691	0.9486
0.2	0.6711	0.7181	0.9258	0.7151	0.7509	0.9404
0.4	0.6443	0.7012	0.9147	0.6913	0.7347	0.9315
0.6	0.6157	0.6853	0.9014	0.6665	0.7195	0.9210
0.8	0.5804	0.6697	0.8824	0.6372	0.7048	0.9064
1.0	0.4967	0.6519	0.8217	0.5740	0.6887	0.8624

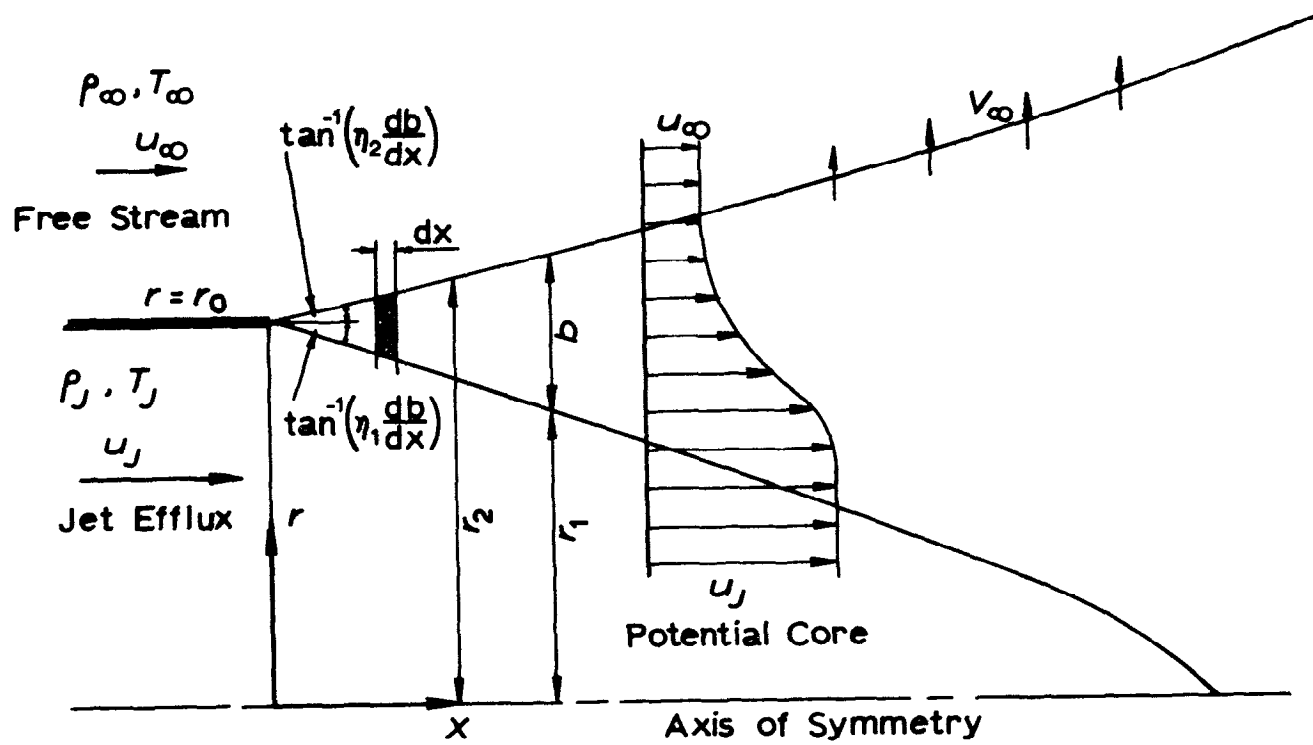


Fig.1 Schematic sketch of the mixing layer region in an axisymmetric jet.

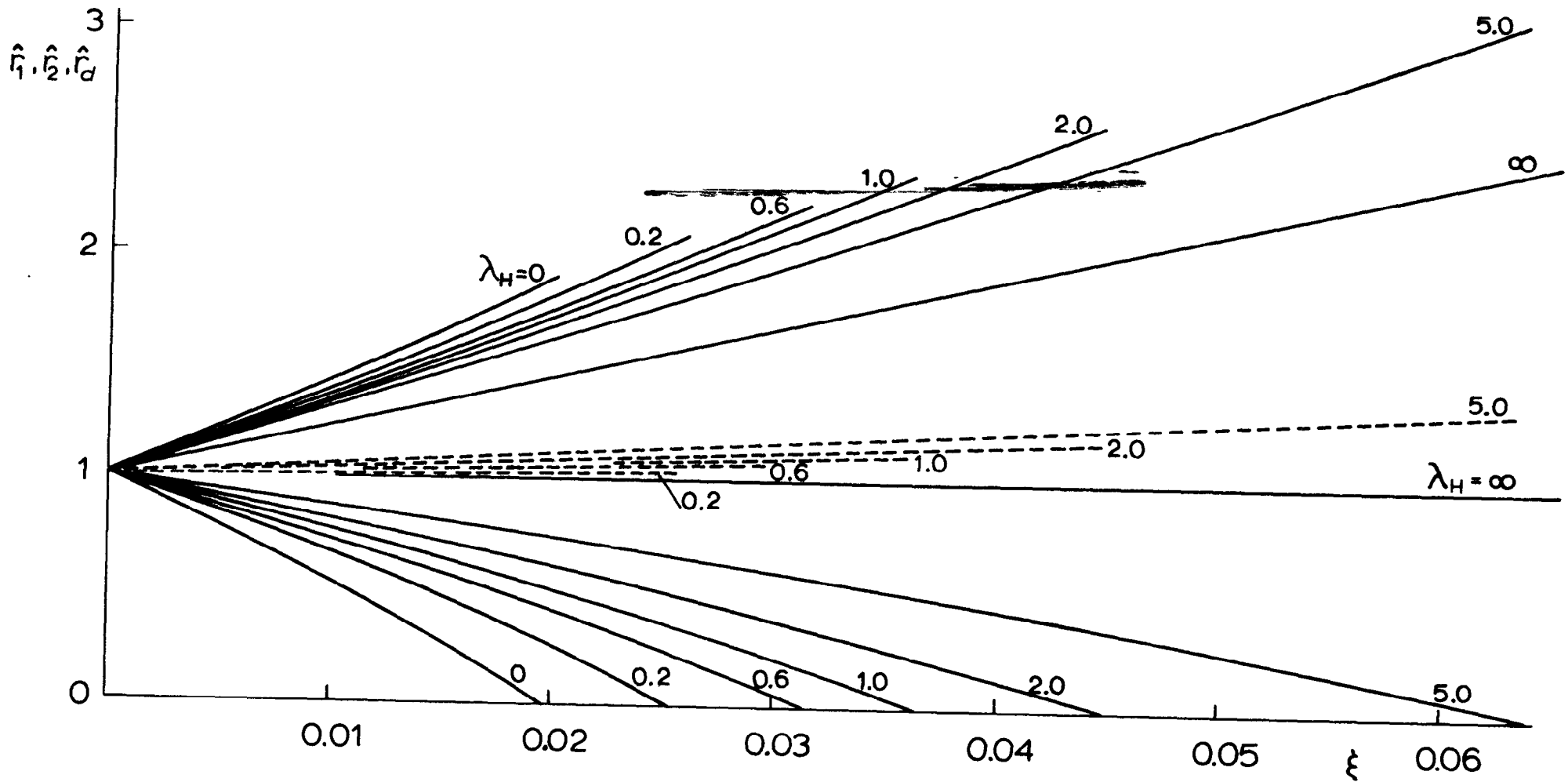


Fig.2 Development of the inner and outer edges and position of the dividing streamline in axisymmetric mixing layers having various values of $T_{O\infty}/T_{OJ}$. $M_J = 0$. $u_\infty = 0$. $\gamma = 1.40$.

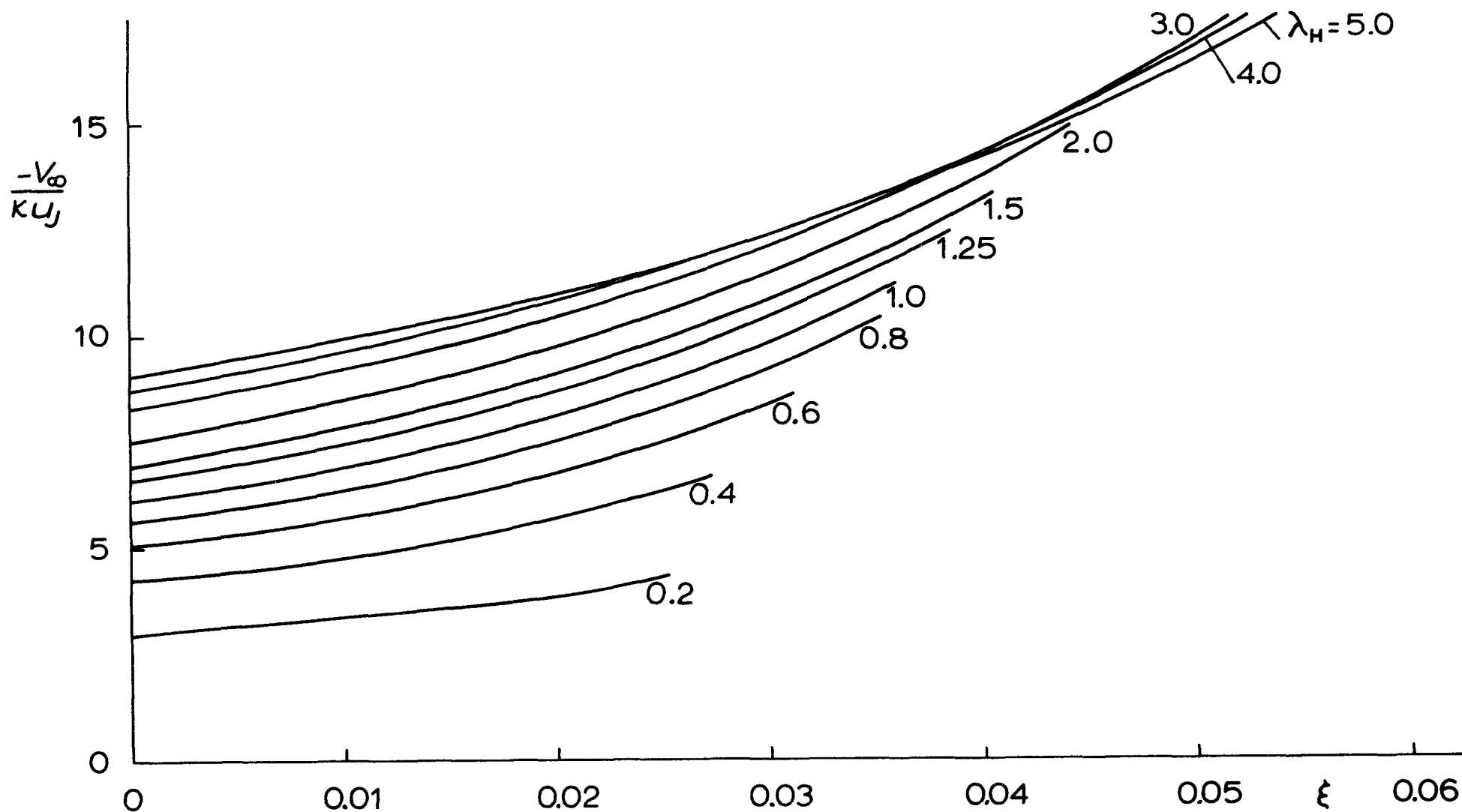


Fig.3 Development of the radial velocity component at the outer edge of an axisymmetric mixing layer for various values of $\lambda_H = T_{0\infty}/T_{0J}$. $M_J = 0$. $u_\infty = 0$. $\gamma = 1.40$.

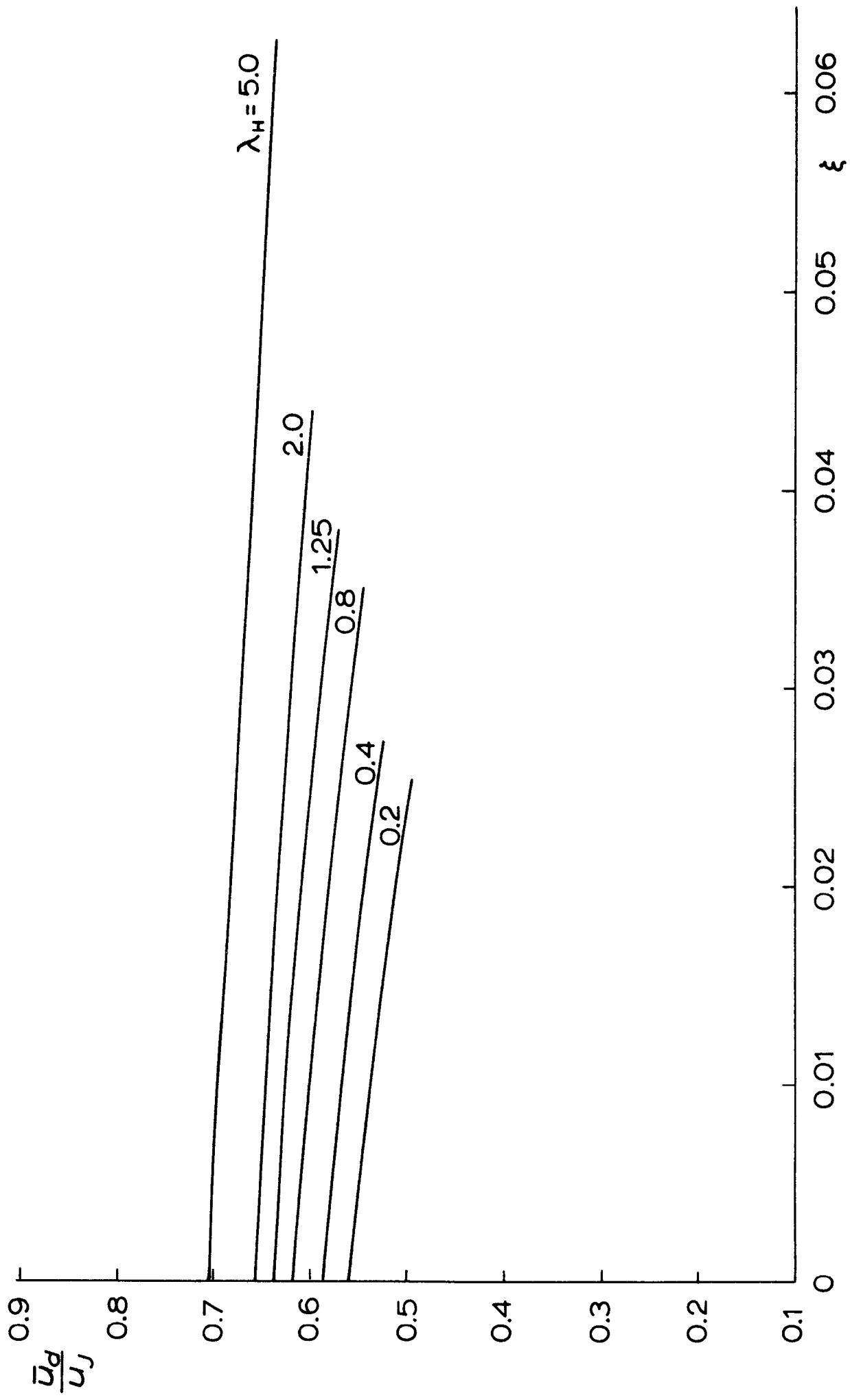


Fig.4 Development of the velocity on the dividing streamline for various values of $\lambda_H = T_{0\infty}/T_{0J}$.
 $M_\infty = 0$. $u_\infty = 0$. $\gamma = 1.40$

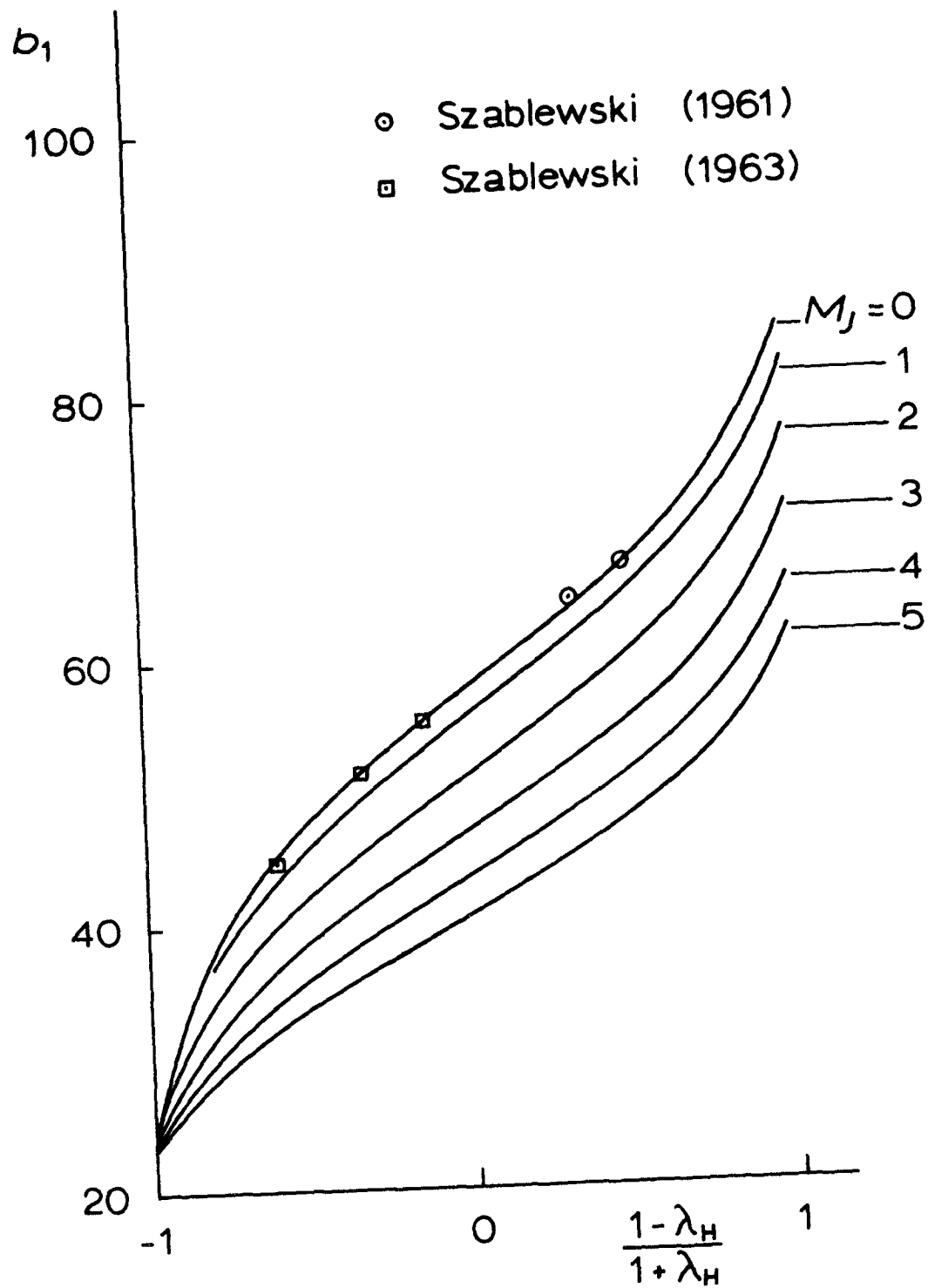


Fig.5 The spreading rate of the mixing layer at $x = 0$
 as a function of λ_H for various values of M_j .
 $u_\infty = 0$. $\gamma = 1.40$.

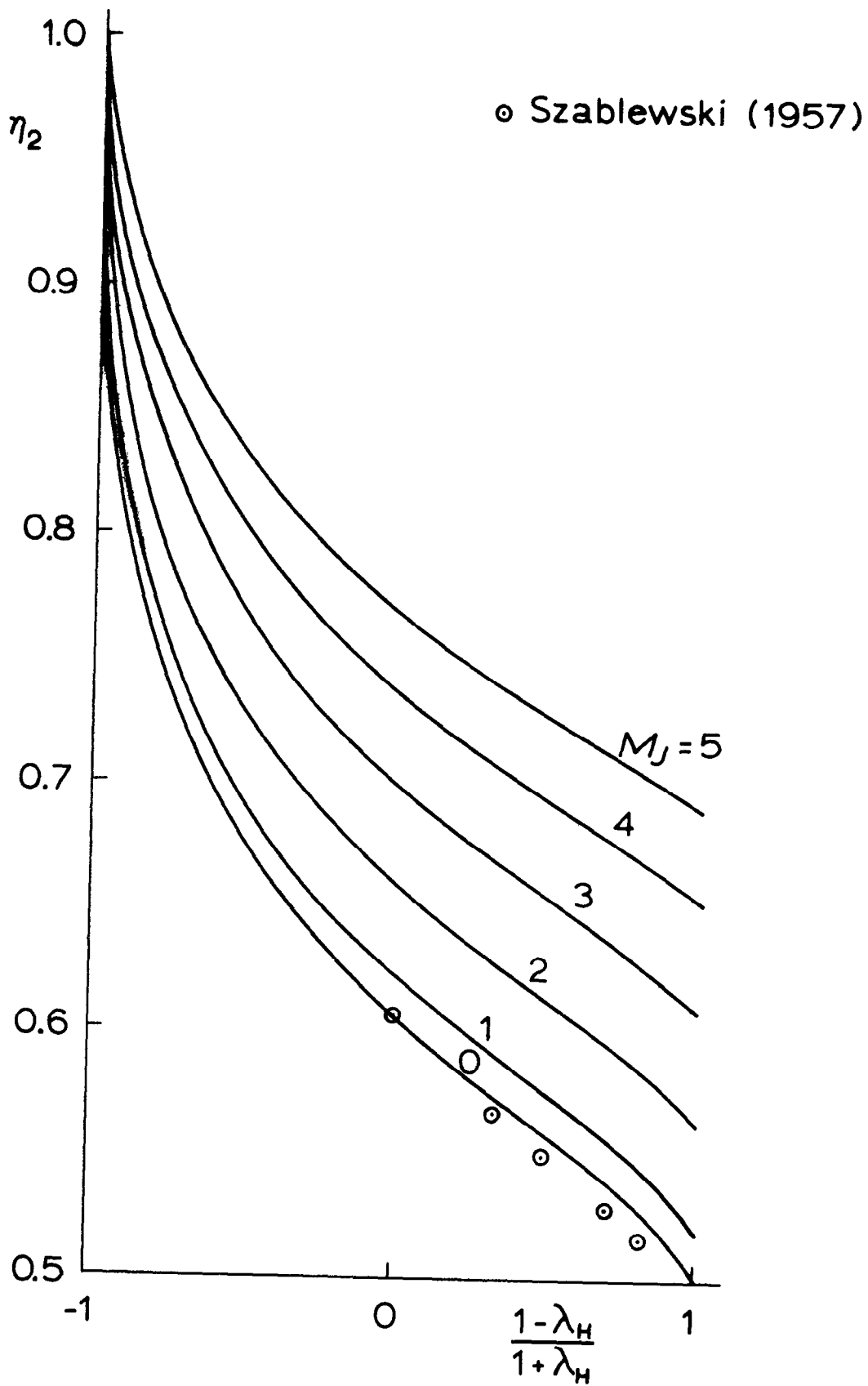


Fig.6 The ratio of $r_2 - r_0$ to b as $x \rightarrow 0$ as a function of λ_H for various values of M_J . $u_\infty = 0$. $\gamma = 1.40$.

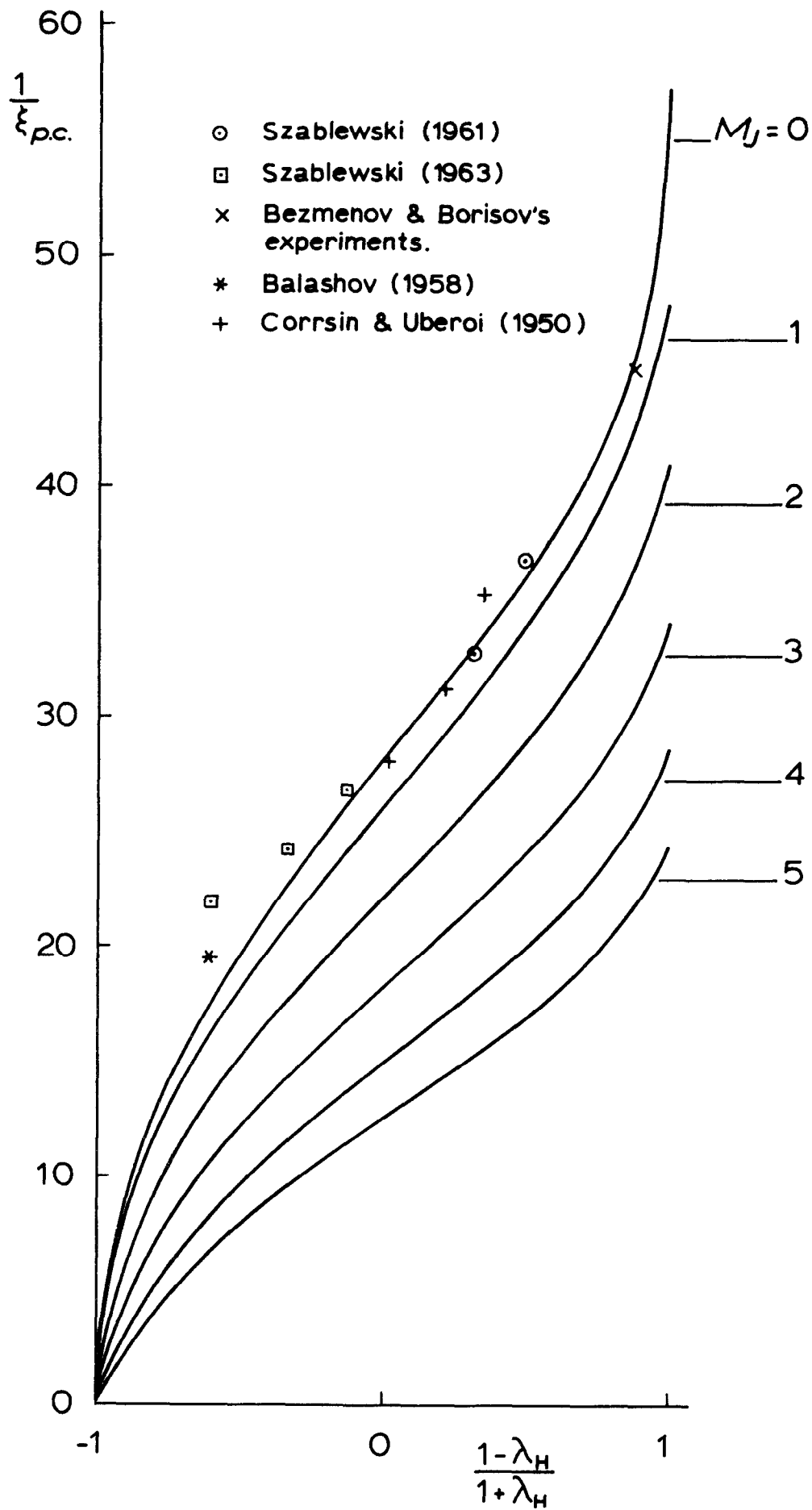


Fig.7 The reciprocal of the potential-core length as a function of λ_H for various values of M_J . $u_\infty = 0$. $\gamma = 1.40$.

Theoretical : $Pr_T = 0.5$

○ Szablewski (1961)

□ Szablewski (1963)

Experimental :

△ Johannesen (1962) $M_J = 1.4$

+ Hill & Nicholson (1964) $M_J = 3.0$

x do. $M_J = 4.0$

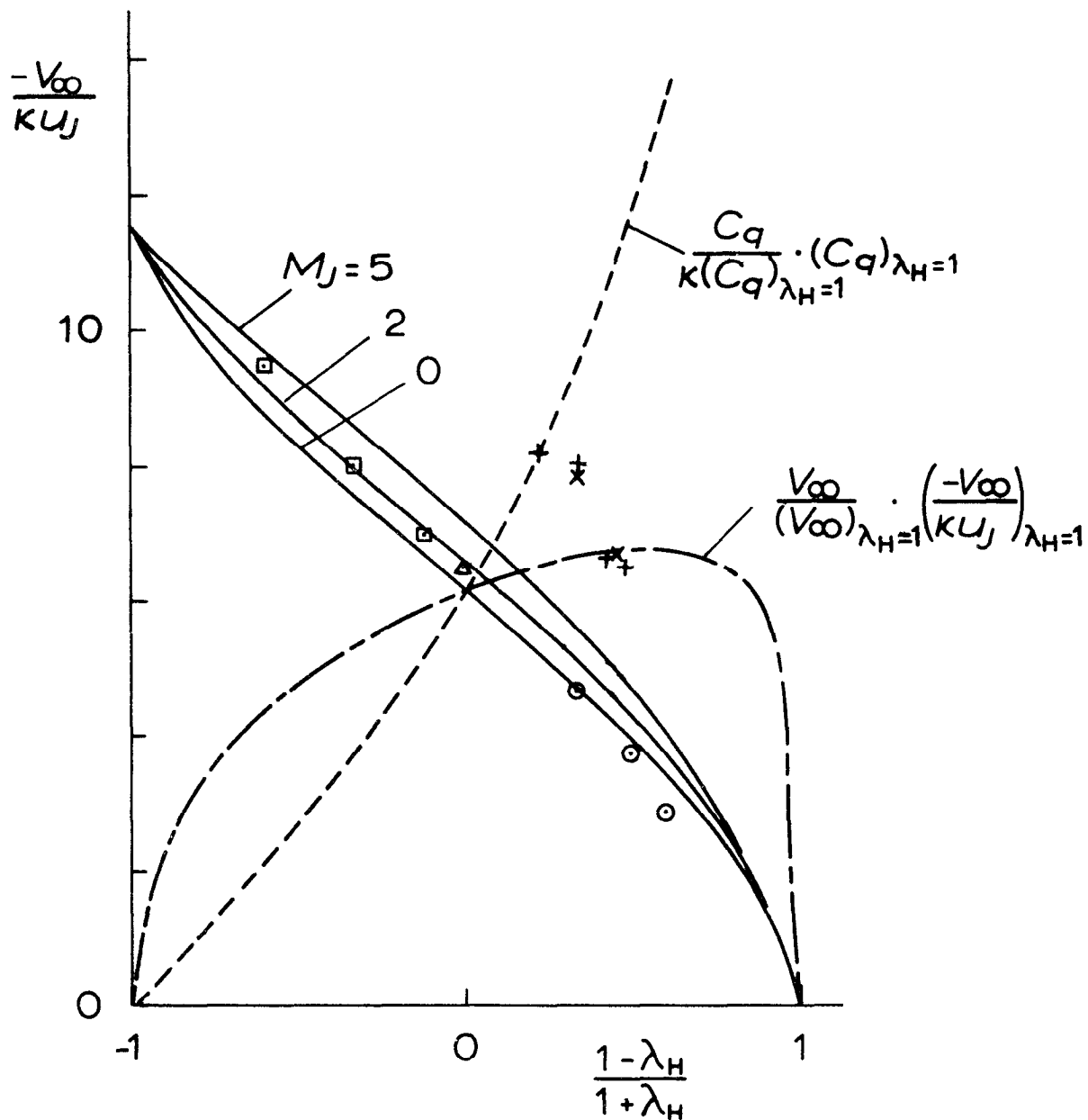


Fig.8 The entrainment velocity at $x = 0$ as a function of λ_H for various values of M_J . $u_\infty = 0$. $\gamma = 1.40$.

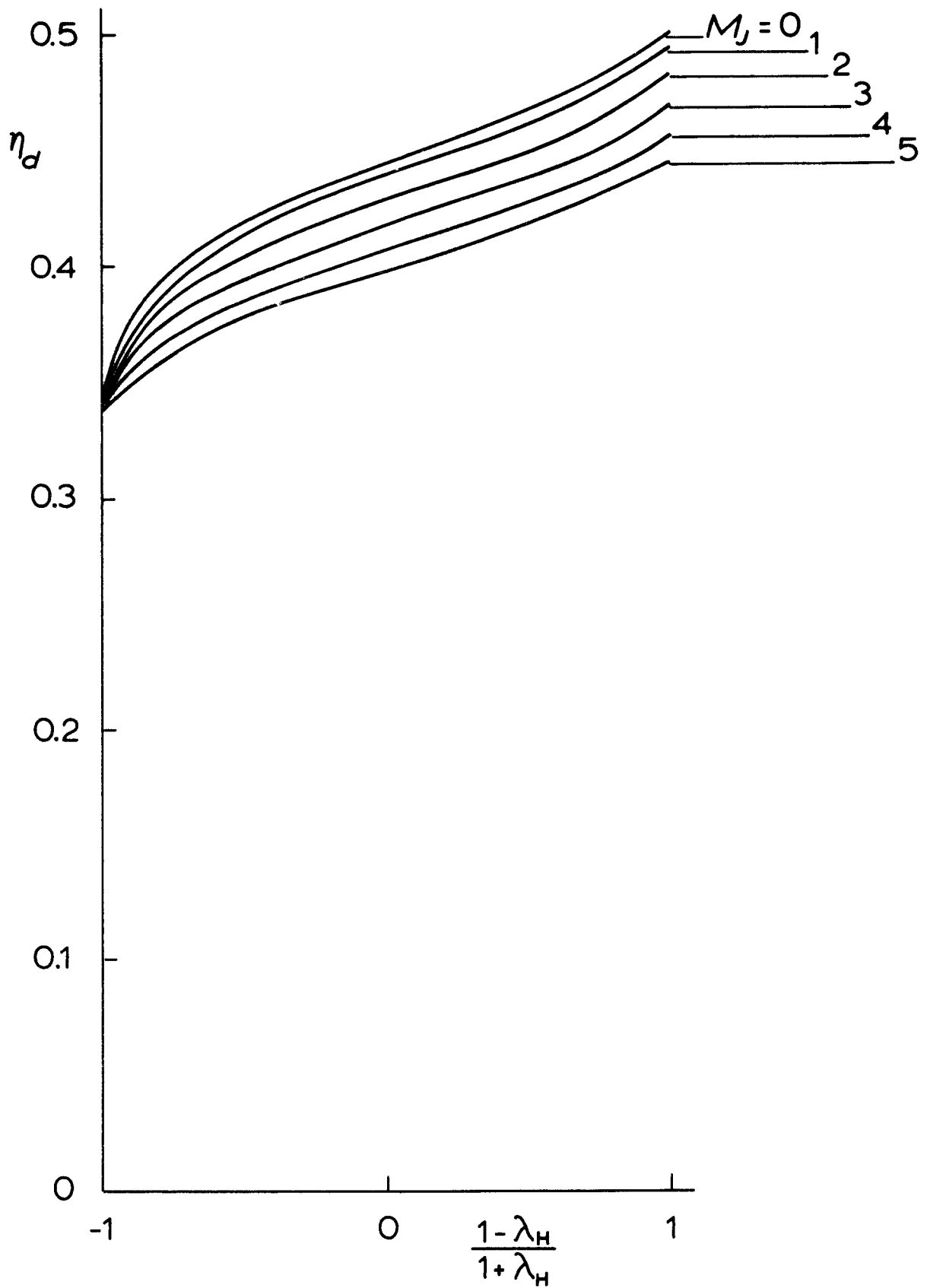


Fig.9 The limit of $(r_d - r_1)/b$ as $x \rightarrow 0$ (i.e. the position of the dividing streamline) as a function of λ_H for various values of M_J . $u_w = 0$. $\gamma = 1.40$.

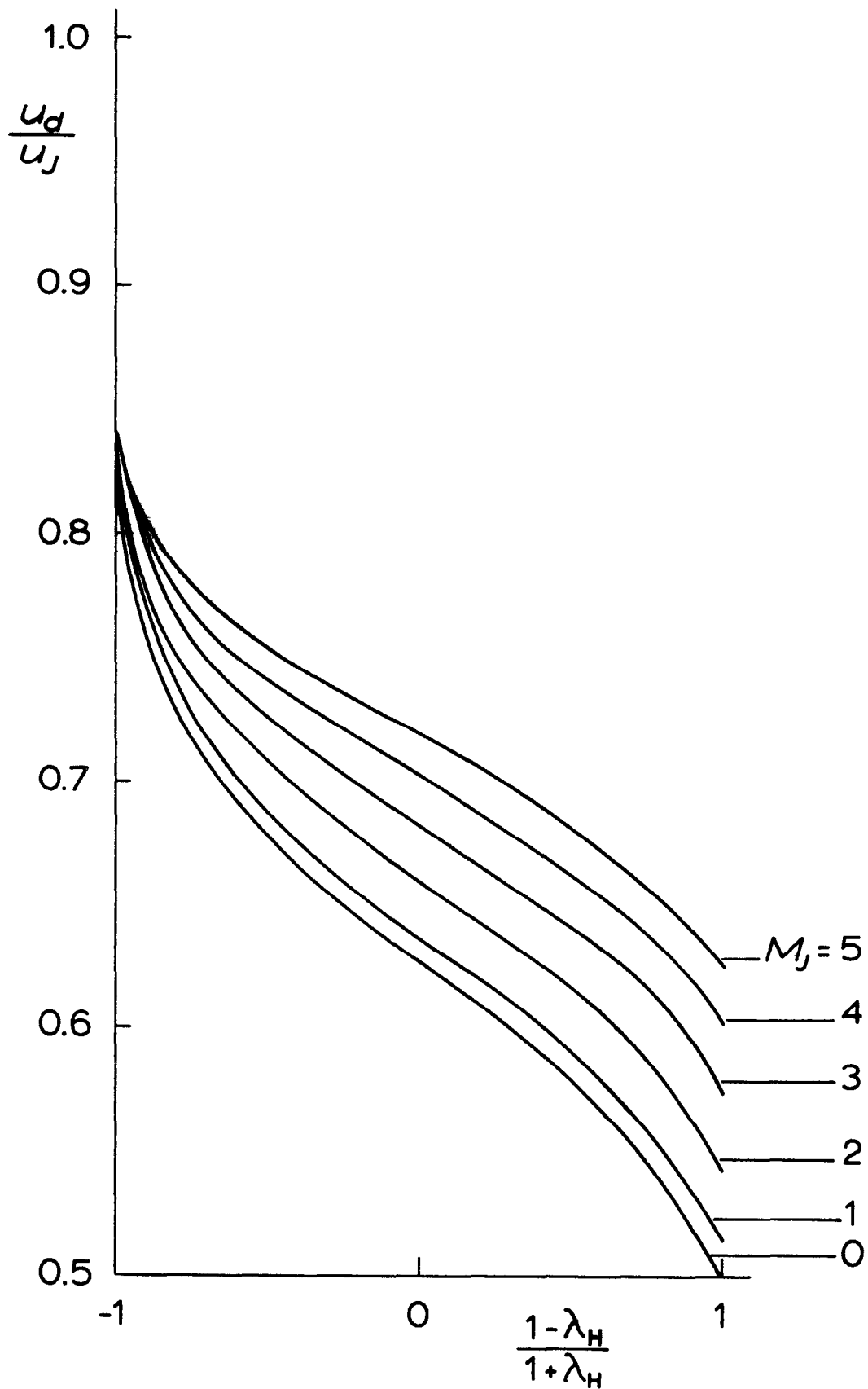


Fig.10 The velocity on the dividing streamline at $x = 0$ as a function of λ_H for various values of M_J . $u_\infty = 0$. $\gamma = 1.40$.

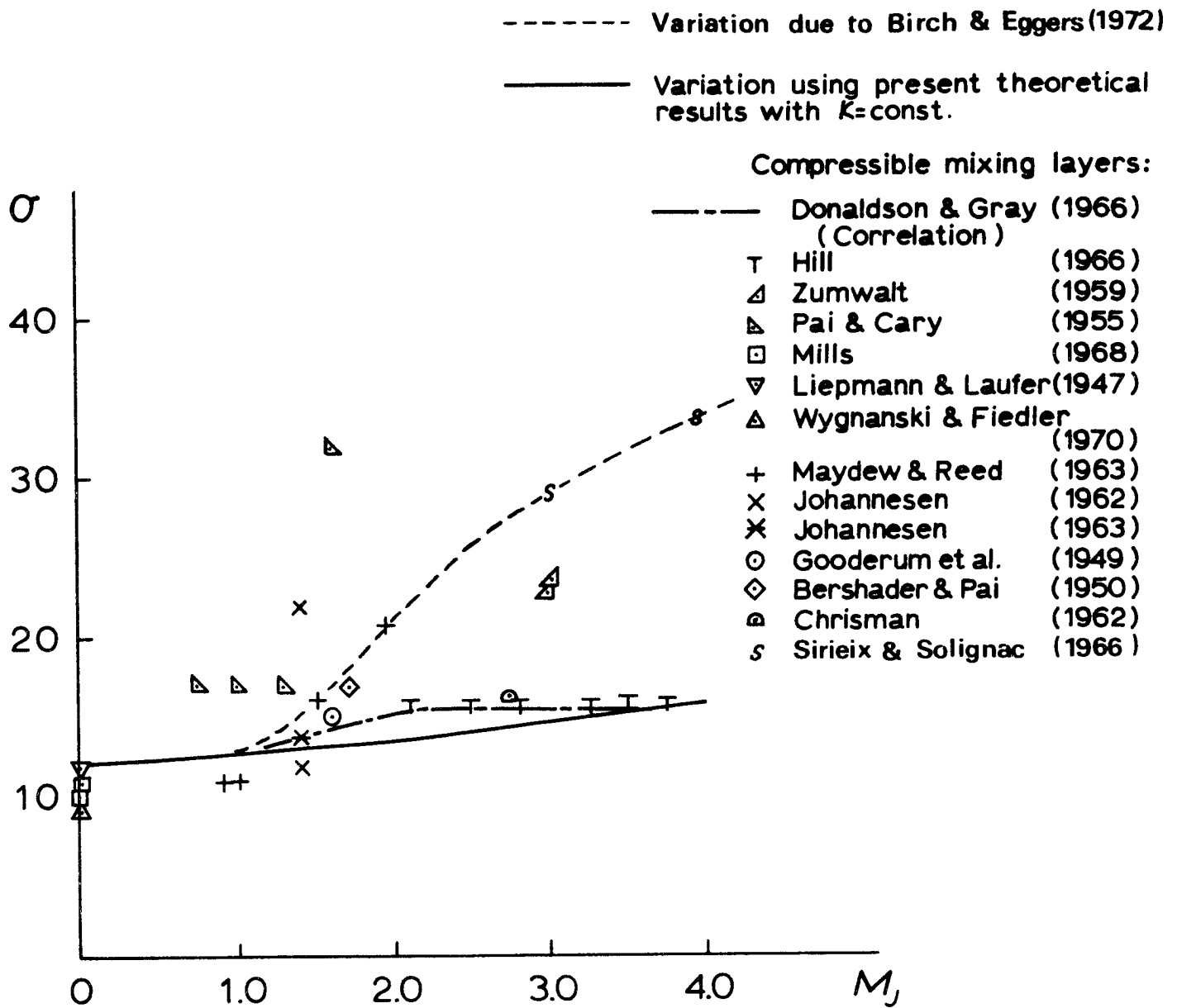


Fig.11 The variation of the spreading parameter with Mach number:
 A comparison between experimental data and theoretical prediction. $\lambda_H = 1$. $u_{\infty} = 0$. $\gamma = 1.40$.

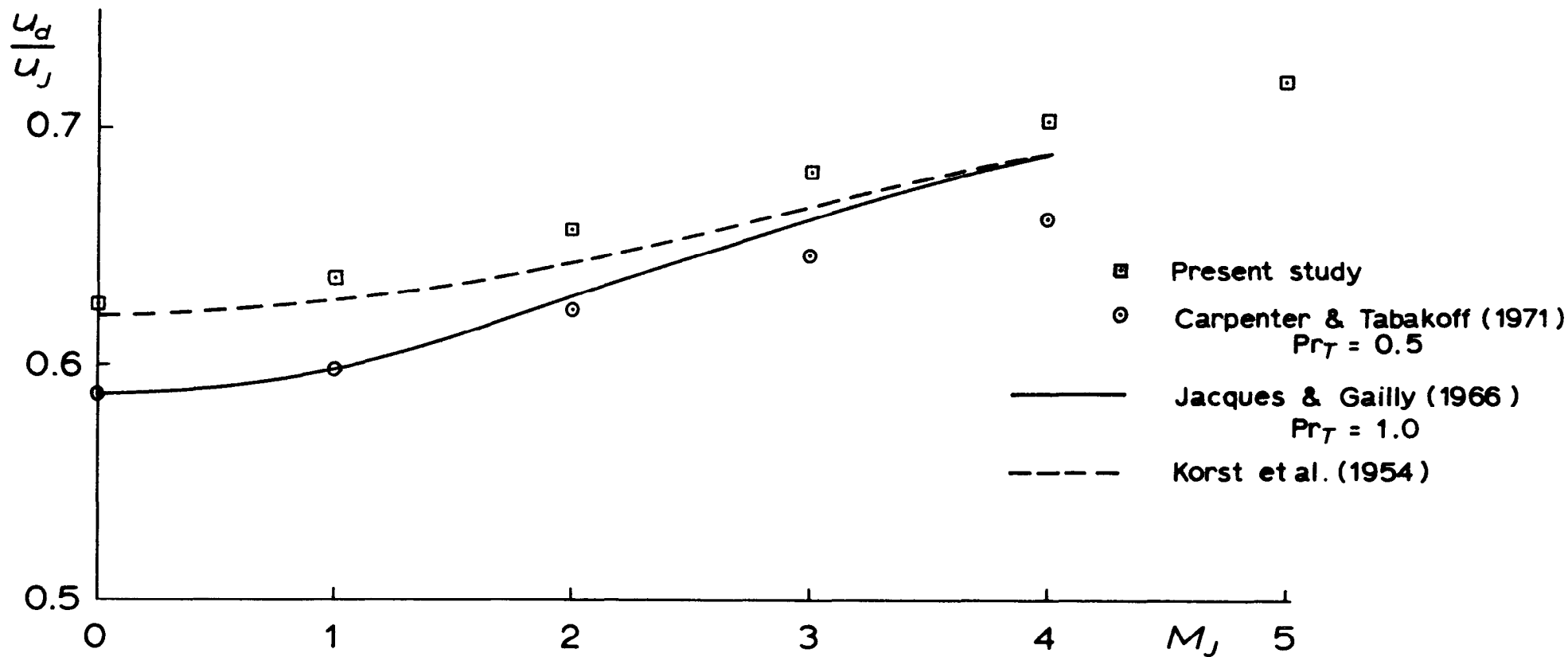


Fig.12 A comparison of various theoretical predictions for dividing streamline velocity as a function of Mach number. $\lambda_H = 1$. $u_m = 0$. $\gamma = 1.40$.

APPENDIX I: APPROXIMATE ANALYTICAL FORMULAE FOR b_1 , Δ_1 , Δ_2 .

Formulae for L_A , J_A and b_1 :

From Equation (4,25) we see that

$$b_1 = -L_A/J_A \quad (A1)$$

$$\text{where } L_A = 2(1-\lambda) \int_0^1 R(dU/d\zeta)^2 d\zeta \quad (A2)$$

$$J_A = \int_0^1 RU(U-\lambda)(U-1)d\zeta \quad (A3)$$

These integrals can be evaluated analytically if we change variables from ζ to U whence

$$L_A = 2(1-\lambda) \int_{1-\epsilon}^{\lambda+\epsilon} R dU/d\zeta dU \quad (A4)$$

$$J_A = \int_{1-\epsilon}^{\lambda+\epsilon} RU(U-\lambda)(U-1)(dU/d\zeta)^{-1} dU \quad (A5)$$

where $\epsilon = 0,01(1-\lambda)$ if the approximate velocity profile (4,13) is used. It also follows from (4,13) that

$$\frac{dU}{d\zeta} = \frac{4k(U-1)(U-\lambda)}{1-\lambda} \quad (A6)$$

where $k = \text{arctanh}(0,98)$ {i.e. $k = k_1/2$ } .

Hence, substitution from eqns, (A6) and (4,7) for $dU/d\zeta$ and R respectively into eqns, (A4) and (A5) leads to the following integrals:

$$L_A = 8k \int_{1-\epsilon}^{\lambda+\epsilon} \frac{(U-1)(U-\lambda)}{(1+m)\{1-\Lambda(1-U)\} - mU^2} dU \quad (A7)$$

$$J_A = \frac{(1-\lambda)}{4k} \int_{1-\epsilon}^{\lambda+\epsilon} \frac{U}{(1+m)\{1-\Lambda(1-U)\} - mU^2} dU \quad (A8)$$

where $\Lambda = (1-\lambda_H)/(1-\lambda)$.

The integrals are readily evaluated to give

$$L_A = \frac{8k}{m} (1-\lambda) - \frac{4k}{m^2} \{(1+m)\Lambda - m(1+\lambda)\} F_1 \\ - \frac{2k}{m^2} \{2m^2\lambda - m(1+m)(1+\lambda)\Lambda + q^2 - 2m(1+m)(1-\Lambda)\} F_2$$

: $m \neq 0$ (A9a)

- (ii) -

$$L_A = -8k \left[\frac{1}{\Lambda^3} \left\{ \frac{1}{2} - \frac{\lambda_T^2}{2} - 2(1-\Lambda)(1-\lambda_T) - (1-\Lambda)^2 \ln(\lambda_T) \right\} \right. \\ \left. - (1+\lambda) \left\{ \frac{(1-\lambda)}{\Lambda} + \frac{(1-\Lambda)}{\Lambda^2} \ln(\lambda_T) \right\} - \frac{\lambda}{\Lambda} \ln(\lambda_T) \right] \\ : m \neq 0, \lambda_H \neq 1 \quad (A9b)$$

$$L_A = \frac{4}{3} k (1-\lambda)^3 \quad : m = 0, \lambda_H = 1 \quad (A9c)$$

where $q = \{(1+m)^2 \Lambda^2 + 4m(1+m)(1-\Lambda)\}^{1/2}$

$$F_1(m, \lambda_H, \lambda) = \ln \left[\frac{(1+m)\{1-\Lambda(1-\lambda-\epsilon) - m(\lambda+\epsilon)^2\}}{(1+m)\{1-\Lambda\epsilon\} - m(1-\epsilon)^2} \right] \approx \ln(\lambda_T)$$

$$F_2(m, \lambda_H, \lambda) = -\frac{2}{q} \left[\operatorname{arctanh} \left\{ \frac{(1+m)\Lambda - 2m(1-\epsilon)}{q} \right\} - \operatorname{arctanh} \left\{ \frac{(1+m)\Lambda - 2m(\lambda+\epsilon)}{q} \right\} \right]$$

and to give

$$J_A = \frac{(1-\lambda)}{4k} \left[-\frac{F_1}{2m} - \frac{(1+m)\Lambda}{2m} F_2 \right] \quad : m \neq 0 \quad (A10a)$$

$$J_A = -\frac{(1-\lambda)}{4k\Lambda} \left\{ (1-\lambda) + \frac{(1-\Lambda)}{\Lambda} \ln(\lambda_T) \right\} \quad : m = 0, \lambda_H \neq 1 \quad (A10b)$$

$$J_A = -(1-\lambda)^2(1+\lambda)/(8k) \quad : m = 0, \lambda_H = 1 \quad (A10c)$$

ϵ has been assumed to be zero to obtain eqns. (A9b & c) and (A10b & c) since this only introduces a very small error in these special cases but makes the formulae very much less cumbersome,

In the special case of $m = 0, \lambda_H = 1$

$$b_1 = -\frac{L_A}{J_A} = 56.3 \frac{(1-\lambda)}{(1+\lambda)} \quad (A11)$$

This agrees with the relationship which Abramovich (1963) deduced by means of a less rigorous dimensional analysis,

Formulae for Δ_1 and Δ_2 :

$$\Delta_1 = \int_0^1 (1-RU) d\zeta \quad \& \quad \Delta_2 = \int_0^1 (1-RU^2) d\zeta \quad (A12)$$

Again we change variables from ζ to U , substitute from eqn. (4.7) for R , and find after a certain amount of algebraic manipulation that

$$\Delta_1 = \frac{(1-\lambda)}{4k} \int_{\lambda+\epsilon}^{1-\epsilon} \left[\frac{\alpha_1}{U-\lambda} + \frac{\gamma_1 U + \beta_1}{(1+m)\{1-\Lambda(1-U)\} - mU^2} \right] dU \quad (A13)$$

where/

where

$$\alpha_1 = \frac{m\lambda + (1+m)(1-\Lambda)}{(1+m)\lambda\Lambda + (1+m)(1-\Lambda) - m\lambda^2} \quad (\text{A14a})$$

$$\beta_1 = \frac{\{m - (1+m)\Lambda + \lambda m\}(1+m)(1-\Lambda)}{(1+m)\lambda\Lambda + (1+m)(1-\Lambda) - m\lambda^2} \quad (\text{A14b})$$

$$\gamma_1 = m\alpha_1 \quad (\text{A14c})$$

and

$$\Delta_2 = \frac{(1-\lambda)}{4k} \int_{\lambda+\epsilon}^{1-\epsilon} \left[\frac{\alpha_2}{U-\lambda} + \frac{\gamma_2 U + \beta_2}{(1+m)\{1-\Lambda(1-U)\} - mU^2} \right] dU \quad (\text{A15})$$

where

$$\alpha_2 = \frac{(1+m)\lambda + (1+m)(1-\Lambda)}{(1+m)\lambda\Lambda + (1+m)(1-\Lambda) - m\lambda^2} \quad (\text{A16a})$$

$$\beta_2 = \frac{\{(1+m)(1-\Lambda) + m\lambda\}(1+m)(1-\Lambda)}{(1+m)\lambda\Lambda + (1+m)(1-\Lambda) - m\lambda^2} \quad (\text{A16b})$$

$$\gamma_2 = m\alpha_2 \quad (\text{A16c})$$

The integrals involved can be readily evaluated to give the following formulae for Δ_1 and Δ_2 ,

$$\Delta_1 = \frac{\alpha_1(1-\lambda)}{2} - \frac{\beta_1(1-\lambda)}{4k} F_2(m, \lambda_H, \lambda) - \gamma_1 J_A \quad (\text{A17a})$$

$$\Delta_2 = \frac{\alpha_2(1-\lambda)}{2} - \frac{\beta_2(1-\lambda)}{4k} F_2(m, \lambda_H, \lambda) - \gamma_2 J_A \quad (\text{A17b})$$

ARC CP No.1345
October 1975
Carpenter, P.W.

A THEORETICAL INVESTIGATION OF HIGH-SPEED
AXISYMMETRIC TURBULENT MIXING LAYERS
WITH LARGE TEMPERATURE DIFFERENCES

A two-parameter integral method is developed for predicting the mean-flow characteristics of high-speed axisymmetric turbulent mixing layers with large temperature differences. Results are presented graphically and in tabular form for such quantities as spreading rate, entrainment velocity, potential-core length and velocity along the dividing streamline. These results are for the case of a jet issuing into a
quiescent/

ARC CP No.1345
October 1975
Carpenter, P.W.

A THEORETICAL INVESTIGATION OF HIGH-SPEED
AXISYMMETRIC TURBULENT MIXING LAYERS
WITH LARGE TEMPERATURE DIFFERENCES

A two-parameter integral method is developed for predicting the mean-flow characteristics of high-speed axisymmetric turbulent mixing layers with large temperature differences. Results are presented graphically and in tabular form for such quantities as spreading rate, entrainment velocity, potential-core length and velocity along the dividing streamline. These results are for the case of a jet issuing into a
quiescent/

ARC CP No.1345
October 1975
Carpenter, P.W.

A THEORETICAL INVESTIGATION OF HIGH-SPEED
AXISYMMETRIC TURBULENT MIXING LAYERS
WITH LARGE TEMPERATURE DIFFERENCES

A two-parameter integral method is developed for predicting the mean-flow characteristics of high-speed axisymmetric turbulent mixing layers with large temperature differences. Results are presented graphically and in tabular form for such quantities as spreading rate, entrainment velocity, potential-core length and velocity along the dividing streamline. These results are for the case of a jet issuing into a
quiescent/

quiescent medium; a range of jet Mach numbers from 0 to 5 is taken. For each Mach number results are presented corresponding to values of the temperature ratio across the mixing layer ranging from 0 to ∞ . On the whole the available experimental data agree well with the theoretical predictions. Results for the case where the jet issues into a moving stream are not presented graphically or in tabular form, but approximate analytical formulae are given whereby most of the quantities of interest may be determined.

quiescent medium; a range of jet Mach numbers from 0 to 5 is taken. For each Mach number results are presented corresponding to values of the temperature ratio across the mixing layer ranging from 0 to ∞ . On the whole the available experimental data agree well with the theoretical predictions. Results for the case where the jet issues into a moving stream are not presented graphically or in tabular form, but approximate analytical formulae are given whereby most of the quantities of interest may be determined.

quiescent medium a range of jet Mach numbers from 0 to 5 is taken. For each Mach number results are presented corresponding to values of the temperature ratio across the mixing layer ranging from 0 to ∞ . On the whole the available experimental data agree well with the theoretical predictions. Results for the case where the jet issues into a moving stream are not presented graphically or in tabular form, but approximate analytical formulae are given whereby most of the quantities of interest may be determined.

© *Crown copyright 1976*

Published by
HER MAJESTY'S STATIONERY OFFICE

To be purchased from
49 High Holborn, London WC1 6HB
13a Castle Street, Edinburgh EH2 3AR
41 The Hayes, Cardiff CF1 1JW
Brazennose Street, Manchester M60 8AS
Southey House, Wine Street, Bristol BS1 2BQ
258 Broad Street, Birmingham B1 2HE
80 Chichester Street, Belfast BT1 4JY
or through booksellers